Modelling forest management within a global vegetation model—Part 2: Model validation from a tree to a continental scale

V. Bellassen [a,*], G. le Maire [b], O. Guin [a], J.F. Dhôte [c,d], P. Ciais [a], N. Viovy [a]

[a] Laboratoire des Sciences du Climat et de l'Environnement, Commissariat à l'énergie atomique, CEA-Orme des Merisiers, F-91191 Gif-sur-Yvette CEDEX, France
[b] CIRAD, Persyst, UPR 80, s/c UMR Eco&Sols, 2 Place Viala - bât 12, 34060 Montpellier cedex 01, France
[c] Direction Technique et Commerciale Bois, Office National des Forêts, Boulevard de Constance, 77300 Fontainebleau, France
[d] INRA, UMR1092 Laboratoire d'étude des Ressources Forêt-Bois, Nancy, France

ABSTRACT

The construction of a new forest management module (FMM) within the ORCHIDEE global vegetation model (GVM) allows a realistic simulation of biomass changes during the life cycle of a forest, which makes many biomass datasets suitable as validation data for the coupled ORCHIDEE-FM GVM. This study uses three datasets to validate ORCHIDEE-FM at different temporal and spatial scales: permanent monitoring plots, yield tables, and the French national inventory data. The last dataset has sufficient geospatial coverage to allow a novel type of validation: inventory plots can be used to produce continuous maps that can be compared to continuous simulations for regional trends in standing volumes and volume increments. ORCHIDEE-FM performs better than simple statistical models for stand-level variables, which include tree density, basal area, standing volume, average circumference and height, when management intensity and initial conditions are known: model efficiency is improved by an average of 0.11, and its average bias does not exceed 25%. The performance of the model is less satisfying for tree-level variables, including extreme circumferences, tree circumference distribution and competition indices, or when management and initial conditions are unknown. At the regional level, when climate forcing is accurate for precipitation, ORCHIDEE-FM is able to reproduce most productivity patterns in France, such as the local lows of needleleaves in the Parisian basin and of broadleaves in south-central France. The simulation of water stress effects on biomass in the Mediterranean region, however, remains problematic, as does the simulation of the wood increment for coniferous trees. These pitfalls pertain to the general ORCHIDEE model rather than to the FMM. Overall, with an average bias seldom exceeding 40%, the performance of ORCHIDEE-FM is deemed reliable to use it as a new modelling tool in the study of the effects of interactions between forest management and climate on biomass stocks of forests across a range of scales from plot to country.

© 2010 Elsevier B.V. All rights reserved.

1. Introduction

Global vegetation models (GVMs) simulate fluxes of carbon, energy and water in ecosystems at the global scale, generally on the basis of processes observed at a plant scale. Despite their correct ability to simulate hourly local (e.g., at flux tower sites) and global seasonal to interannual (e.g., compared with atmospheric CO_2 observations) variations in CO_2 fluxes, these models usually fall short of simulating biomass and soil carbon pool dynamics within ecosystems (Desai et al., 2007; Viovy et al., 2010; Carvalhais et al., 2010). This shortcoming has been attributed to forest age structure

and management, which are not simulated by most GVMs (Ciais et al., 2008). ORCHIDEE-FM, a new GVM with an explicit representation of forest management practices typical of European forests (Bellassen et al., 2010), addresses this challenge, but it has yet to be validated against independent datasets.

Several of the many variables processed by GVMs can be measured and, thus, used for validation: for example, leaf area index (Demarty et al., 2007), light absorption and light use efficiency (Jung et al., 2007), carbon stocks (Masek and Collatz, 2006), evapotranspiration (Thornton et al., 2002), and latent and sensible heat fluxes (Abramowitz et al., 2008). However, validation exercises for GVMs most frequently focus on carbon fluxes estimated with eddy-covariance techniques (Thornton et al., 2002; Krinner et al., 2005; Turner et al., 2005; Schaefer et al., 2008).

Flux towers have two major strengths: the flux data that they deliver have a very fine resolution in time, often half-hourly, and their reasonably large footprint of approximately 100 ha (Nagy et

* Corresponding author. Tel.: +33 1 69 08 31 01.
E-mail addresses: valentin.bellassen@lsce.ipsl.fr, vbella@lsce.ipsl.fr
(V. Bellassen).

al., 2006; Reichstein et al., 2007) averages the variability due to individual trees. With regard to GVM validation, they also have two major drawbacks. First, their costly structure and maintenance limits their numbers: large networks such as FLUXNET manage to have good coverage of the different land-use types and climates (Baldocchi et al., 2001), but they seldom provide clear insights on inter-site variability within a given climate and land-use type. Therefore, it is difficult to generalise measurements that could be heavily influenced by local conditions (e.g., soil fertility or hydrological parameters) or management (e.g., recent thinning) (Lindner et al., 2004). Second, because eddy-covariance technology is quite recent, the time-series are seldom longer than one decade (Urbanski et al., 2007). This precludes the validation of full stand rotations, which commonly last between 100 and 200 years, on temperate forest ecosystems (Bottcher et al., 2008) unless flux towers are smartly distributed to measure chronosequences (Amiro et al., 2006).

Thus, in their review of terrestrial carbon models, Hurtt et al. (1998) concluded that GVMs need to be validated for a diverse range of spatial and temporal scales. Datasets of forest stand structure variables (e.g., height, basal area, and volume increment) are good candidates for this diversification because they are often available on wider spatial and temporal scales than eddy-covariance data, but these variables are not simulated by most GVMs. A new generation of GVMs that explicitly simulate forest management begins to bridge this gap: Desai et al. (2007) validated the regional forest biomass simulated by Ecosystem Demography with data derived from forest inventories in the midwest United States, and Sato et al. (2007) compared the local age structure simulated by SEIB-DGVM with intensive monitoring plots. However, to date, no GVM has been evaluated simultaneously at the diverse spatial and temporal scales relevant to managed forests.

Beyond the assessment of model error, a model validation exercise also provides the opportunity for a better understanding of the model's strengths and pitfalls. In particular, it should be designed to attribute a share of model error to each model component. One way of attributing this model error is to quantify the improvement of model fit when a given component is switched on. This approach was used by Zaehle et al. (2006) for a model component simulating the processes involved in the age-related decline of net primary productivity (NPP). Because it requires a validation variable that is simulated both in the absence and presence of the component, this method is not always applicable. Another way of attributing modelling error is to force a model by replacing the outputs of one model component by site measurements. By assimilating a satellite-derived leaf area index (LAI) in ORCHIDEE, Demarty et al. (2007) showed that the phenology component of the model is responsible for 25% of the lack of fit to flux tower data. Because the new forest management module (FMM) of ORCHIDEE generates a whole new set of variables and processes, this second approach was found to be better suited to discriminate between its error and the error coming from the general core of ORCHIDEE.

In this study, we use forestry datasets to further evaluate the performance of the ORCHIDEE-FM simultaneously at several spatial and temporal scales, which are all relevant to the novelty introduced by the forestry management module, namely the simulation of stand structure and its evolution with age. Two requirements are set for a validation dataset:

- It should cover the diverse spatial and temporal scales necessary for exploring regional variations and the full lifespan of a forest from harvest to harvest.
- It should provide the possibility to replace the input of ORCHIDEE to the FMM with actual field values so that a share of modelling error can be attributed to both the ORCHIDEE and the FMM components (see Fig. 1).
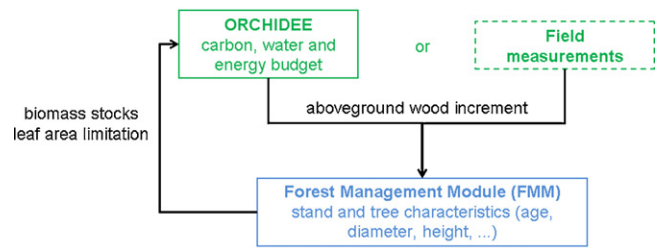

Fig. 1. ORCHIDEE-FM: coupled or forced with field measurements. Wood increment can be simulated by the core of ORCHIDEE or derived from site measurements. The management module simulates its allocation to individual trees in the stand and computes mortality (self-thinning, anthropogenic thinning or clear-cutting) based on a density index.

No single dataset was found to match all of these requirements. Instead, we selected three complementary datasets: permanent forest monitoring plots, yield tables, and extensive forest inventory data (see Fig. 2). Permanent plots provide long time series and detailed within-plot measurements, but their spatial coverage is very limited. Yield tables cover the entire European continent, but their precise area of relevance and source data are often unknown. Inventory data is sufficiently abundant to create spatially continuous maps of carbon stocks and stock changes (through surface tree cores), but only one snapshot measurement is available for each plot. Here, these datasets are successively compared to specific simulations to validate ORCHIDEE- and to identify the most important sources of model error.

The notion of model validation is controversial (Oreskes et al., 1994). Confirmation that models reproduce existing *in situ* measurements reasonably well is, nevertheless, required of GVMs, the projections of which are used in the definition of climate change mitigation and adaptation policy (IPCC, 2007). Therefore, we use the term of "validation" with the cautionary requirements set by Rykiel (1996), clearly specifying the model's purpose, its context of operation and the criteria that it must meet for being considered "acceptable for use":

- Model purpose: to simulate the age-related dynamics of carbon stocks and fluxes that are ignored in the standard version of ORCHIDEE.
- Context of operation: a tree to continental scale, limited to Europe.
- Validation criteria: whereas plot-scale models, calibrated with site- and species-specific parameters, can be expected to fit local data series, the aim of a GVM is to simulate a regional aver-
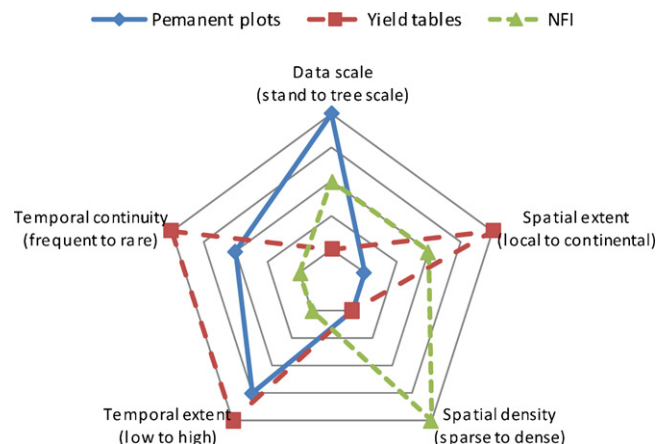
Fig. 2. Characteristics of the three datasets used.

age CO_2 flux, typically using 0.5° resolution. The performance of ORCHIDEE-FM is, therefore, assessed through its ability to cut across a cloud of data points corresponding to different sites in the same region.

All abbreviations used in this paper are indexed in Appendix A.

2. Material and methods

2.1. ORCHIDEE and its forest management module (FMM)

2.1.1. Description of ORCHIDEE-FM

The ORCHIDEE global vegetation model (ORganising Carbon and Hydrology In Dynamic Ecosystems) was designed to operate from regional to global scales (Krinner et al., 2005). ORCHIDEE typically represents an average mature forest at steady-state equilibrium in a *big-leaf* manner. For a given climate, it simulates the carbon, water and energy budget at the pixel scale. For carbon, ORCHIDEE computes its fixation (gross primary productivity or GPP), allocates photosynthetates to the different biomass compartments where they are respired or stored, and recycles carbon through constant tree mortality and soil respiration. To simulate forest management, several processes have been added to the standard version of ORCHIDEE, among which is a forest management module (FMM) inspired by the stand-level model FAGACEES (Dhôte and Hervé, 2000). The key concept is to add to the "average tree" representation of ORCHIDEE an explicit distribution of individual trees, which is the basis for a process-based simulation of mortality (see Fig. 1). The above-ground plot-scale wood increment simulated by ORCHIDEE is distributed among individual trees according to the rule of Deleuze et al. (2004):

$$\delta ba_i = \frac{\gamma}{2} \times \left(circ_i - m \times \sigma + \sqrt{(m \times \sigma + circ_i)^2 - 4 \times m \times \sigma \times circ_i} \right) \tag{1}$$

where δba_i is the annual increase in the basal area of tree i in square meters, and $circ_i$ is the circumference of tree i in meters. γ, σ and m are the slope, the threshold and the smoothing parameters, respectively (see Figure S1): trees whose circumference is lower than σ grow very little; thus, γ is the slope of the δba_i vs. the $circ_i$ relationship above σ.

Then, tree mortality processes, due to natural competition, anthropogenic thinning or clear-cutting, rely on the self-thinning rule (Eq. (2)) of Reineke (1933).

$$dens_{max} = \frac{\alpha_{st}}{Dg^{\beta_{st}}} \tag{2}$$

where $dens_{max}$ is the stand maximum density in ind ha^{-1} (individuals per hectare); α_{st} and β_{st} are parameters; and Dg is the quadratic mean diameter in m.

For more information on the structure of ORCHIDEE-FM, see Bellassen et al. (2010).

2.1.2. Pedo-climatic inputs and model "spinup"

The climate data used in this study to drive ORCHIDEE is from the 0.25°-resolution REMO reanalysis covering the 1861–2007 period (Kalnay et al., 1996; Vetter et al., 2008). Maps of soil depth and texture were derived from FAO and IGBP products (Vetter et al., 2008). Following a standard method in GVM modelling, a model "spinup" is performed before all simulations to define the initial conditions from which subsequent simulations will be performed, in particular for soil carbon. For this "spinup", ORCHIDEE and ORCHIDEE-FM are repeatedly run for the climate of the years 1861–1911 with a CO_2 concentration of 280 ppm until all ecosystem carbon and water pools reach a cyclical (clearcut-regrowth) steady-state equilibrium.

The conditions of the stand after the last clearcut are used as initial conditions for all ORCHIDEE-FM simulations.

2.2. Validation data

Three complementary datasets are used to validate the FMM and its integration in ORCHIDEE: permanent plots, yield tables and national inventory. All three are necessary to cover the three different scales of interest: tree scale (e.g., individual tree growth and circumference distribution), stand scale (e.g., tree density and basal area), and continental scale (e.g., inter-regional variations). The following paragraphs describe each dataset and its specific use in our model validation assessment. Table 1 summarises the characteristics and aims of each simulation. Figure S4, Figure S5, and Figure S9 summarise measurements, simulations and validated variables for each of the three datasets. The uncertainty associated to each dataset in discussed in part 2 of Supplementary Materials.

2.2.1. Permanent plots

2.2.1.1. Description. Fifty-eight permanent plots (PP) were set by the *Institut National de la Recherche Agronomique* (INRA) for long-term monitoring of the evolution of forest stands (Dhôte and Hervé, 2000). These plots contain either oaks or beeches. They all belong to even-aged stands and were subject to different management intensities with a post-thinning relative density index (*rdi*, see Eq. (3)) ranging from 0.4 (heavy thinning) to 1 (no anthropogenic thinning = unmanaged).

$$rdi = \frac{dens}{dens_{max}} \tag{3}$$

where *rdi* is the relative density index, and *dens* and $dens_{max}$ are the actual and maximal tree densities, respectively, of the stand in ind ha^{-1}. $dens_{max}$ is derived from Eq. (2). All trees in the plots are marked, and for each measurement year, the status of trees is recorded (dead, alive, or thinned), as is their circumference at breast height. Measured ages span 37–203 years, with an average measurement frequency of 4.2 years.

A summary of permanent plot characteristics is provided in Appendix B.

2.2.1.2. Estimation of non-measured variables. The key variables of interest available at each plot for the validation of the FMM-simulated counterparts are as follows:

- circumference distribution variables: minimum, average, and maximum circumference as well as number of trees in a given circumference class,
- stand variables: tree density and basal area.

Other variables, such as standing volume, standing biomass, tree height, wood increment, and individual tree growth indicators (the σ and γ of Eq. (1)) can be estimated. For detailed information on the estimation method, see part 1 of Supplementary Materials.

2.2.1.3. PP$_f$ and PP$_c$ simulations: validation of tree-scale and stand-scale characteristics. The PP$_f$ (permanent plot-forced) simulation is aimed at validating tree-scale and stand-scale characteristics between two measured states: the state of a stand at first measurement and its state at last measurement. To validate the FMM separately from the rest of ORCHIDEE, the annual increase in above-ground woody biomass ($wood_{inc}$) is forced by the *in situ* estimate instead of the value simulated by the core of ORCHIDEE. The initial conditions of PP$_f$ are the conditions of each permanent plot at its first measurement regarding tree circumferences and, therefore, aboveground biomass. The other biomass compartments (e.g.,

Table 1

Simulations summary. Variable abbreviations: *dens* (tree density), *ba* (basal area), av_{circ} (average circumference), $circ_{min}$ (minimum circumference), $circ_{max}$ (maximum circumference), *distrib* (circumference distribution), σ (threshold circumference for basal area growth), γ (competition index), vol_{tot} (total wood volume produced), vol_{th} (cumulated thinned wood volume), NPP_{woody} (annual wood increment), vol_{main} (standing wood volume).

Simulation	Dataset	Model used	Source of woody NPP	Initial conditions	Time period	Validated variables
PP_f	Permanent plots	FMM	Data	Data	First measurement → last measurement	$dens$, ba, av_{circ}, $circ_{min}$, $circ_{max}$, $distrib$, σ, γ
PP_c	Permanent plots	ORCHIDEE-FM	Model	Data	First measurement → last measurement	$dens$, ba, av_{circ}, $circ_{min}$, $circ_{max}$, σ, γ, vol_{tot}
PP_{ic}	Permanent plots	FMM	Data	Model	Year 0 → first measurement	$dens$, ba, av_{circ}, $circ_{min}$, $circ_{max}$
YT_f	Yield tables	FMM	Data	Model	Year 0 → year 80	$dens$, ba, dom_{height}, av_{height}, av_{circ}, vol_{main},
NFI_{std}	National Forest Inventory	ORCHIDEE	Model	Model	1876, 1916, 1956 → 2006	NPP_{woody}, vol_{main}
NFI_{fmm}	National Forest Inventory	ORCHIDEE-FM	Model	Model	1876, 1916, 1956 → 2006	$NPPwoody$, $volmain$
NFI_{opt}	National Forest Inventory	ORCHIDEE-FM, optimised photosynthesis	Model	Model	1876, 1916, 1956 → 2006	NPP_{woody}, vol_{main}
NFI_{st}	National Forest Inventory	ORCHIDEE-FM, self-thinning only	Model	Model	1876, 1916, 1956 → 2006	NPP_{woody}, vol_{main}

leaves, roots, and soil) are not used as inputs in the FMM and, therefore, do not need to be accounted for when the FMM is forced.

The aim of the PP_c (permanent plot-coupled) simulation is to assess the additional error brought to the FMM outputs by an initial error in the simulation of stand-scale wood increment by ORCHIDEE. PP_c is therefore similar to PP_f, except that the FMM is no longer forced by data-derived $wood_{inc}$. Instead, the coupled ORCHIDEE-FM model is run over the measurement period of each plot using the corresponding climate forcing to provide a simulated $wood_{inc}$. Whereas the differences between PP_f and the data reveal the error of the FMM in simulating management and growth distribution, those between PP_c and PP_f reflect the error due to the simulation of $wood_{inc}$ by ORCHIDEE. Comparing the performance of PP_f vs. *data* to that of PP_c vs. PP_f allows us to attribute a share of the total error (PP_c vs. *data*) to each of the model's components. Comparing PP_c directly to the data would be confusing because the error of each component might cancel each other out and, consequently, be wrongly interpreted as a high modelling efficiency.

2.2.1.4. PP_{fi} simulation: validation of initial distribution. The PP_f (permanent plots initial conditions) simulation complements the PP_f simulation by assessing the model's ability to reproduce the state of each plot at its first measurement, starting from the default model initial conditions of 10,000 trees per hectare, with circumferences following a decreasing exponential distribution (Bellassen et al., 2010). The FMM is, therefore, run on each permanent plot from its date of regeneration until the first measurement year. For the PP_f simulation, the FMM is decoupled from the rest of ORCHIDEE: the annual increase in aboveground woody biomass between year 1 and the first measurement is forced by the average annual wood increment estimated from field data over the measured period.

2.2.2. Yield tables

2.2.2.1. Description. More than a thousand forest yield tables have been compiled by the Joint Research Centre (JRC, 2009). They cover 26 European countries and 23 genuses. Forest yield tables give the evolution of typical stand variables, including tree density, basal area, dominant or average height, average circumference, standing volume and thinned volume, with age. All of these variables will be tested against FMM simulations for validation. Yield tables are usually established based on either permanent plots monitored over an entire rotation, or temporary plots of different ages monitored once. Their aim is to reproduce the average growth pattern of a tree species in a given region, which sometimes declines in *yield classes* representing different levels of treatment or local fertility. Because the FMM simulates the growth of an average coniferous

or broadleaf species managed as a high stand, coppices and fast-growing poplars and eucalypts were discarded from the database. When needed, cormometric volume (merchantable volume) was converted into dendrometric volume (whole tree) using a branch to total volume ratio of 0.25 for needleleaf species and 0.38 for broadleaf species (Loustau, 2004).

2.2.2.2. Testing the effect of climate and management in the dataset. Yield tables complement permanent plots by providing a presumably much more diverse range of climates, species and management conditions. However, neither management style nor climate are represented by explicit indicators as is the case with permanent plots for which accurate location, plot age and the targeted relative density index play that role. A first step in testing the FMM against this assumed variety of climates and management conditions is therefore to test whether climate and management effects can indeed be detected in the dataset. To test the climate effect, an analysis of variance was performed using the mixed linear model of Eq. (4).

$$vol_{tot}(i, j, k) = \alpha + \beta_i + \gamma_j + \varepsilon(i, j, k) \tag{4}$$

where α is the intercept; β_i and γ_j are the coefficients associated with plant functional type (PFT) i and country j, respectively, and $vol_{tot}(i, j, k)$, and $\varepsilon(i, j, k)$ are the total volume produced at year 80 and the error term associated with yield table k of PFT i and country j, respectively. The error terms $\varepsilon(i, j, k)$ are assumed to be dependent upon PFT and country, justifying the use of a linear mixed model with PFT and country as fixed effects.

Because the total biomass (standing biomass + thinned biomass) produced by a plot is largely independent of the management style (Lanier, 1994), this variable was not suited to test the diversity of management styles in the data. For this purpose, a second analysis of variance based on tree density was performed using the linear mixed model of Eq. (5).

$$dens(i, j, k) = \alpha + \beta_i + \gamma_j + \delta \times vol_{tot}(i, j, k) + \varepsilon(i, j, k) \tag{5}$$

where α is the intercept; β_i, γ_j and δ are the coefficients associated with plant functional type (PFT) i, country j, and total volume produced at year 80, respectively; $dens(i, j, k)$, $vol_{tot}(i, j, k)$ and $\varepsilon(i, j, k)$ are the density, the total volume produced at year 80 and the error term associated with yield table k of PFT i and country j, respectively. The error terms $\varepsilon(i, j, k)$ are assumed to be dependent upon PFT and country, justifying the use of a linear mixed model.

Density is highly dependent on management for a given productivity level, which is embedded in the random factor vol_{tot}, and management is, therefore, likely to explain most of the variance attributed to country and PFT when productivity is already cap-

tured by another variable (here vol_{tot}). In this model, β and γ can thus be interpreted as indicators of the country- and PFT-specific variation in management style.

2.2.2.3. YT_f simulation: validation of stand-scale characteristics across Europe.

The YT_f (yield tables-forced) simulation is aimed at validating stand-scale characteristics across Europe. As in the PP_f simulation, the annual increase in aboveground biomass is forced by the mean annual increment given in the yield table to validate the FMM separately from the rest of the ORCHIDEE model. However, because the yield tables do not provide initial conditions with enough detail, the initial conditions of the YT_f simulation are set to the default model initial conditions, as in the PP_{fi} simulation. To bridge the data gap between age 0 and the first age of the yield table, which varies between 5 and 20 years, the mean annual increment during this period is set to add up to the first data on total volume.

2.2.3. French national inventory

2.2.3.1. Description.
The French National Forest Inventory (NFI) conducts yearly field measurement campaigns covering the entire French metropolitan territory. Each intersection of a systematic grid of 10 km × 10 km is photo-interpreted to determine land cover and land-use. Of these intersections, every other forested point, totalling about 8000 points per year, is visited and inventoried following the NFI protocol (IFN, 2006): circumference at breast height, width of the last five rings, height and species are recorded for a representative sample of trees. NFI allometric rules are used to estimate tree volume and annual volume increment, and all of these data provide the basis for an estimate of plot-scale tree density, basal area, dominant height, standing volume and the annual volume increment. For even-aged stands, a few trees are cored to the stem centre to estimate stand age. For this study, we pooled together the results of three campaigns (2005, 2006 and 2007). Because the FMM only represents even-aged high stands, all other management types were excluded from the analysis. Our sample size was, therefore, reduced to 11,222 sites. The raw data are available on the IFN website: www.ifn.fr.

2.2.3.2. Interpolation.
Both permanent plots and yield tables are unsuitable to test the ability of ORCHIDEE-FM to simulate regional trends in carbon stocks and fluxes. Thus, a spatially continuous dataset is needed. With its high spatial density, the NFI dataset presents the opportunity to build continuous maps: for the category of broadleaf plots of the 80–100 years age class alone, half the French territory has at least 10 plots within a distance of 0.5° (55 km), and only 24% of the territory has less than 5 plots. However, this dataset is heterogeneous: the order of magnitude of the standard deviation of the volume increment within a radius of 0.5° is 30%. Therefore, a smoothing is necessary to eliminate the local variations due to topography, soil fertility and species composition and to retain only the regional climate-related variations in carbon stocks and fluxes. Several interpolation techniques were tested to obtain these smoothed data-derived maps, resulting in the joint use of the following two methods:

- *Large footprint interpolation technique*: the data were interpolated with a minimum footprint radius of 0.5° and no distance weighting. Where necessary, the footprint was extended to include a minimum of 10 plots. The result is a 0.05° resolution map for which each final pixel represents the average of all plots within a 0.5° radius of the centre of the pixel.
- *Data density mask*: density masks were created to distinguish pixels with more than 10 plots within a 0.5° radius. Applying these masks restricts model-data comparisons to the areas where the uncertainty in the data is lowest.

2.2.3.3. NFI_{std} and NFI_{fmm} regional simulations.
Two types of simulations were conducted to assess the model's ability to reproduce the trends observed in the NFI data.

- The NFI_{std} simulation aims at representing an average forest at steady-state equilibrium, typical of GVMs. Thus, the standard version of ORCHIDEE was run between 1956 and 2006, which is the average measurement year for the dataset (2005–2007).
- The three NFI_{fmm} simulations aim at validating the coupled version of the ORCHIDEE-FM. The model was run for 50, 90, and 130 years with all runs ending in 2006. The resulting NFI_{fmm50}, NFI_{fmm90}, and NFI_{fmm130} results can, thus, be compared to NFI plots of three selected age-classes: 40–60 years, 80–100 years and 120–140 years. In both cases, the CO_2 concentration follows its historical increase from 290 ppm in 1876 to 378 ppm in 2006.

The wood increment estimated in the NFI data comes from surface cores of live trees. It is a gross commercial wood increment, and it does not account for woody losses from artificial thinning or natural mortality. From the simulation of tree-level growth and mortality, a similar variable can be extracted from the ORCHIDEE-FM simulations, allowing its validation. The commercial wood increment is converted to the total wood increment using the relevant PFT-specific branch expansion factor (BEF) of IPCC (2003). "Difference maps" present the relative difference between each pixel of data-derived maps and its closest simulation point. These maps are limited to pixels complying with the data density masks, which are pixels with at least 10 inventory plots within a 0.5° radius of the centre of the pixel.

2.2.3.4. NFI_{opt} and NFI_{st} simulations for error attribution.
Unlike permanent plots, it is not possible to estimate the history of productivity in each NFI plot. The only data point available is the average tree-ring width over the previous 5 years that is obtained from a surface core. Therefore, attributing error to the management or productivity simulation is not straightforward when one is looking at cumulative variables such as standing biomass. To do so, two additional types of simulations are performed:

- For the NFI_{opt} simulations, we replaced the default values of the photosynthesis efficiency parameters (vc_{max}, the maximum capacity of the Rubisco enzyme, and vj_{max}, the maximum regeneration speed of the Rubisco enzyme) with the values of Santaren (2006), who optimised their ORCHIDEE model based on eddy-covariance measurements from six European sites. Broadleaves were unaffected, but the photosynthesis efficiency of needle-leaves was increased by 20%. NFI_{opt} simulations are a sensible variant of NFI_{fmm} simulations for productivity.
- For the NFI_{st} simulations, artificial thinning is disabled, and only self-thinning occurs, thus representing the minimal level of management. When a lack of fit between the ORCHIDEE-FM and data for standing biomass comes from overly intensively simulated management, NFI_{st} provides a comparison with the most extensive type of management.

2.3. Criteria of model performance

Two common criteria are used to evaluate model performance: *EF*, model efficiency, and *AB*, model average relative bias (Soares et al., 1995; Smith et al., 1997). Their definition is given by Eqs. (6) and (7).

$$EF = 1 - \frac{\sum_i (mes_i - sim_i)^2}{\sum_i (mes_i - \overline{mes})^2} \tag{6}$$

$$AB = \frac{1}{n} \sum_{i=1}^{n} \frac{sim_i - mes_i}{mes_i} \qquad (7)$$

where mes_i and sim_i are the measured data point i and its simulated counterpart, respectively; $\overline{mes}$ is the data average; and n is the number of data points.

EF reflects the ability of the model to reproduce the data: the closer it gets to 1, the better the fit. AB indicates whether the model has a systematic bias. Whereas an efficient model necessarily has a small systematic bias, the reverse is not always true. However, when a large-scale model such as ORCHIDEE is compared to plot-scale measurements, avoiding systematic bias may be more important than scoring high efficiency: large-scale models are not expected to reproduce each stand specifically but rather to simulate an "average stand" within the gridcell of interest.

To improve the interpretation of these criteria, we undertook three complementary analyses:

- "Shadow models": for each simulation, we built a "shadow model" for ORCHIDEE-FM. These "shadow models" are simple statistical models using the same input variables as ORCHIDEE-FM. For the stand-scale variables of the PP_f simulation, for example, the main input variables of ORCHIDEE-FM are total volume, initial conditions (initial median circumference), and management intensity (post-thinning relative density index). The shadow model thus follows Eq. (8).

$$mes(i) = a \times vol_{tot}(i) + b \times med_{circ}(i) + c \times rdi_{target}(i) + \varepsilon(i) \qquad (8)$$

where mes is the measured variable of interest (e.g., tree density and standing volume); vol_{tot} is the total volume of the stand at the last measurement; med_{circ} is the median circumference of the stand at the first measurement; rdi_{target} is the post-thinning relative density index; a, b, c, and d are regression coefficients; i is the permanent plot number; and $\varepsilon(i)$ is the error term associated with $mes(i)$.

"Shadow models" are calibrated on one half of the dataset, and their efficiency (EF_{stat}) is assessed on the other half. The details of each model and its calibration are presented in Supplementary Materials.

- Systematic vs. unsystematic error: to assess the importance of the average bias, we computed the systematic ($RMSEs$) and unsystematic ($RMSEu$) errors of Willmott (1982), defined by Eqs. (9) and (10), respectively:

$$RMSEs = \frac{1}{n} \sqrt{\sum_{i=1}^{n} (pred_i - mes_i)^2} \qquad (9)$$

$$RMSEu = \frac{1}{n} \sqrt{\sum_{i=1}^{n} (pred_i - sim_i)^2} \qquad (10)$$

where $RMSEs$ and $RMSEu$ are the systematic and unsystematic root mean square error, respectively; n is the number of the measurement; sim is the simulated variable; mes is the measured variable; i is the measurement number; and $pred$ is the value predicted by the linear regression $sim = f(mes)$: $pred_i = a + b \times mes_i$, where a and b are the regression coefficients.

$RMSEs$ represents the error due to a systematic bias in the model, and $RMSEu$ represents the "random" error. The $RMSEs/RMSEu$ ratio places the average relative bias in perspective: even a large AB is not very meaningful if the $RMSEs/RMSEu$ ratio is lower than one.

- Error share of a given model component: an index (ES_{fmm}) of the share of the total error of ORCHIDEE-FM that can be attributed to the FMM component was computed based on the permanent plots data as well as the PP_f and PP_c simulations (see Eq. (11)).

$$ES_{fmm} = \frac{1 - EF_{PPf}}{(1 - EF_{PPf}) + (1 - EF_{PPc})} \qquad (11)$$

where ES_{fmm} is the error share of the FMM model component (0 when all of the error comes from ORCHIDEE and 1 when it comes entirely from the FMM), and EF_{PPf} and EF_{PPc} are the efficiency of PP_f to reproduce the data and the efficiency of PP_c to reproduce the PP_f simulation, respectively.

3. Results

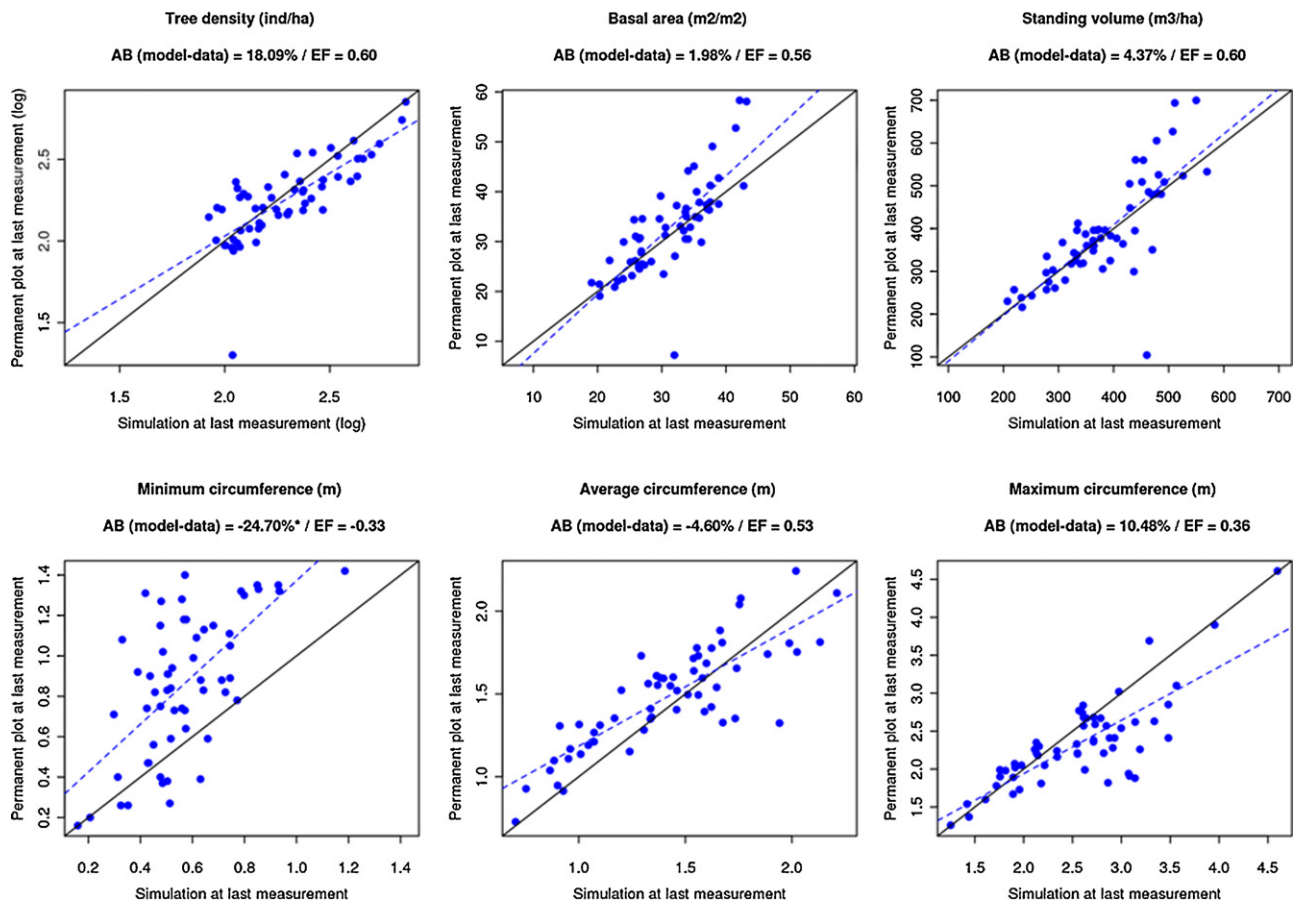### 3.1. Stand scale: stand characteristics

3.1.1. Permanent plots
3.1.1.1. PP_f and PP_{fi} simulations: good performance of the FMM under controlled conditions. Average stand characteristics such as tree density, basal area, average circumference and standing volume are efficiently simulated under the control conditions of PP_f (Figs. 3 and 4). All of these characters have modelling efficiencies higher than 0.5 and average biases below 20%. This average bias is negligible because the systematic error is smaller than the unsystematic error: all $RMSEs$ to $RMSEu$ ratios are lower than 0.6 (Table 2). The model is not as accurate for extreme circumferences: both have lower efficiencies, and the minimum circumference is consistently underestimated with an average bias of −25% and a systematic error component overtaking the unsystematic component. These deficiencies essentially occur for plots with large trees (Fig. 3).

With the approximations necessary for the PP_{fi} simulation (default model initial distribution and average growth rate), the fit of all variables deteriorate. Except for standing volume and average circumference, all model efficiencies become negative. From the results of the PP_{fi} simulation, we conclude that the model could not correctly reach the initial state of the PP_f simulation. Average biases are also higher than for the PP_f simulation, although none exceeds 45%. However, because all $RMSEs$ to $RMSEu$ ratios remain below 0.7, the default initial conditions of ORCHIDEE-FM can be considered to induce no strong systematic bias to the simulations. For both simulations, the FMM is more efficient than its simple statistical "shadow model". For stand-scale variables, its efficiency is on average of 0.11 higher for PP_f and 0.6 higher for PP_{fi}.

3.1.1.2. PP_f and PP_c simulations: a minor share of modelling error for the FMM component. The (inaccurate) simulation of wood increment by ORCHIDEE is a more important source of error than the processes simulated by the FMM. For most variables, the forced FMM (PP_f) is more efficient at reproducing the data than ORCHIDEE-FM (PP_c) is at reproducing the forced FMM (Fig. 4). For basal area, which is the variable most commonly estimated by forest inventories, the efficiency of the forced FMM to reproduce the data is three times higher than that of ORCHIDEE-FM to reproduce the forced FMM, giving an ES_{fmm} value of only 35% (Table 3). Because the efficiency of the coupled PP_c remains quite high for standing volume, the error for this variable is, therefore, split evenly between ORCHIDEE and the FMM ($ES_{fmm} = 48\%$).

3.1.2. Yield tables
3.1.2.1. Statistically significant effect of climate and management practices in the dataset. The statistical model of Eq. (4) explains 64% of the total variance, and both country and PFT predictors have a significant effect (p-value < 0.001) on the total volume produced (the detailed statistics are provided in Supplementary Materials). Therefore, the effect of climate is present, though blurred, in the yield table dataset. This result can be ascertained visually from

Fig. 3. Validation of stand characteristics: PP_f simulation. Each blue dot corresponds the state of one permanent plot at its last measurement. The dotted blue line represents their linear regression. *AB* and *EF* are average relative bias and model efficiency, respectively. An "*" indicates that the systematic error is higher than the unsystematic error (*RMSEs* > *RMSEu*). (For interpretation of the references to color in this figure legend, the reader is referred to the web version of the article.)
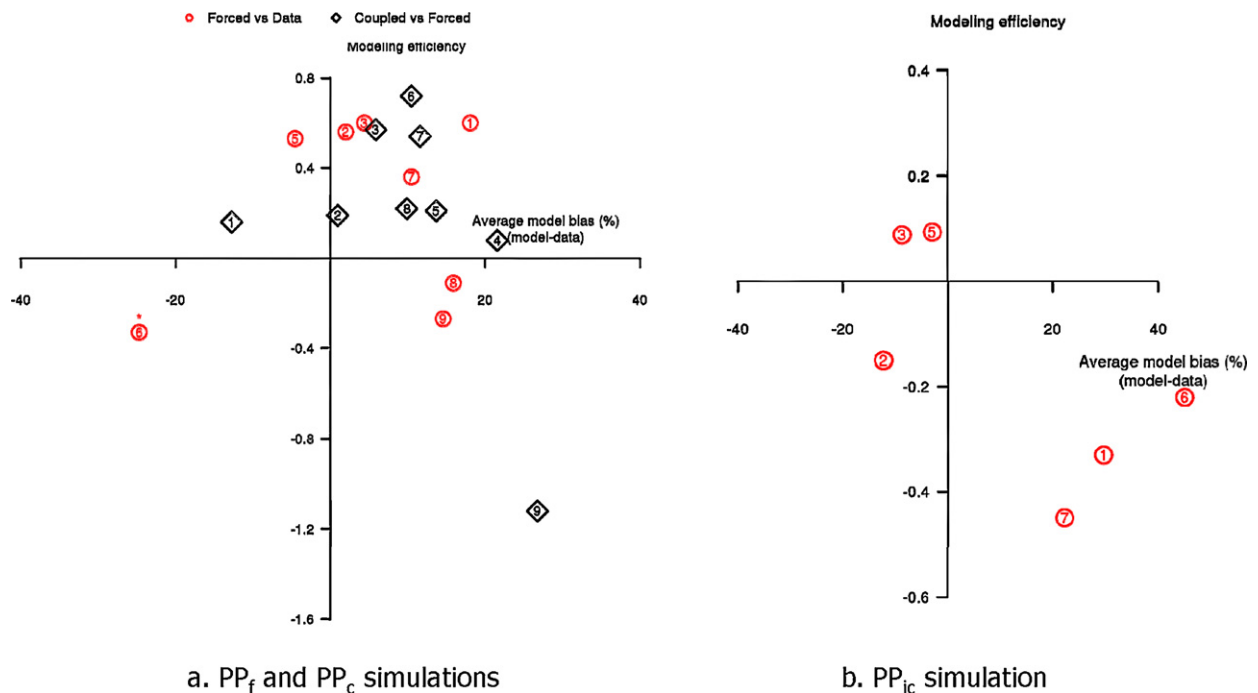
Fig. 4. Summary diagrams of model performance for *PP* simulations. These diagrams represent model efficiency and average bias for a selected set of stand variables. Red circles indicate the ability of the FMM forced with the local wood increment to reproduce data (*PP_f* vs. data and *PP_fi* vs. data), whereas black diamonds indicate the ability of the FMM coupled with the wood increment from ORCHIDEE to reproduce the "forced" simulation (*PP_c* vs. *PP_f*). An "*" indicates that the systematic error is higher than the unsystematic error (*RMSEs* > *RMSEu*). (1) Tree density, (2) basal area, (3) standing volume, (4) total volume, (5) average circumference, (6) minimum circumference, (7) maximum circumference, (8) sigma, (9) gamma. (For interpretation of the references to color in this figure legend, the reader is referred to the web version of the article.)

Table 2

Efficiencies and average biases of PP and YT simulations. Modelling efficiency of ORCHIDEE-FM (EF), modelling efficiency of the relevant statistical model (EF_{stat}), average bias (AB), and systematic/unsystematic error ratio ($RMSEs/RMSEu$) for three validations. Variable abbreviations: *dens* (tree density), *ba* (basal area), av_{circ} (average circumference), $circ_{min}$ (minimum circumference), $circ_{max}$ (maximum circumference), *distrib* (circumference distribution), σ (threshold circumference for basal area growth), γ (competition index), vol_{tot} (total wood volume produced), vol_{th} (cumulated thinned wood volume), NPP_{woody} (annual wood increment), vol_{main} (standing wood volume).

Validation	Variable name	EF	EF_{stat}	AB	AB_{stat}	$RMSEs/RMSEu$
PP_f vs. data	*dens*	0.6	0.40	18%	1%	0.40
	ba	0.56	0.29	2%	10%	0.43
	vol_{main}	0.6	0.39	4%	9%	0.15
	av_{circ}	0.53	0.77	−5%	6%	0.57
	$circ_{min}$	−0.33	0.36	−25%	46%	1.30
	$circ_{max}$	0.36	0.67	10%	−3%	0.67
	σ	−0.11	−0.14	16%	72%	0.69
	γ	−0.27	0.01	15%	4%	0.91
PP_{fi} vs. data	*dens*	−0.33	−0.29	30%	2%	0.02
	ba	−0.15	−0.90	−12%	13%	0.13
	vol_{main}	0.09	−1.59	−9%	18%	0.18
	av_{circ}	0.09	0.10	−3%	0%	0.10
	$circ_{min}$	−0.22	0.05	45%	10%	0.30
	$circ_{max}$	−0.45	−1.24	22%	30%	0.10
PP_c vs. PP_f	*dens*	0.16	na	−13%	na	0.72
	ba	0.19	na	1%	na	0.68
	vol_{main}	0.57	na	6%	na	0.77
	vol_{tot}	0.08	na	22%	na	0.85
	av_{circ}	0.21	na	14%	na	0.81
	$circ_{min}$	0.72	na	10%	na	0.94
	$circ_{max}$	0.54	na	12%	na	1.09
	σ	0.22	na	10%	na	1.05
	γ	−1.12	na	27%	na	1.00
YT_f vs. data	*dens*	−8	−0.08	161%	96%	0.83
	av_{circ}	−0.67	0.48	−18%	−7%	0.78
	ba	0.52	0.41	10%	13%	0.33
	dom_{height}	0.32	0.63	−9%	4%	0.62
	av_{height}	−0.85	0.60	−35%	0%	1.33
	vol_{main}	0.83	0.82	−2%	16%	0.44
	vol_{th}	0.45	0.81	54%	−3%	0.96

Fig. 5: the estimated coefficients for country (γ_j), representing the relative effect of each country corrected for PFT effects, present a climatic pattern with lower values in arid Spain and the cold Russo-Scandinavian countries. This pattern is clearly blurred over western and central Europe, where the differences between countries are difficult to explain based on climate alone.

The statistical model of Eq. (5) explains 47% of the total variance, and all explanatory variables (country, PFT, and total volume produced) have a significant effect (p-value < 0.01) on stand density. The effect of the total volume produced is, as expected, more important than that of PFT and country (F-value is about 50 times higher for total volume). Because management style is expected to vary
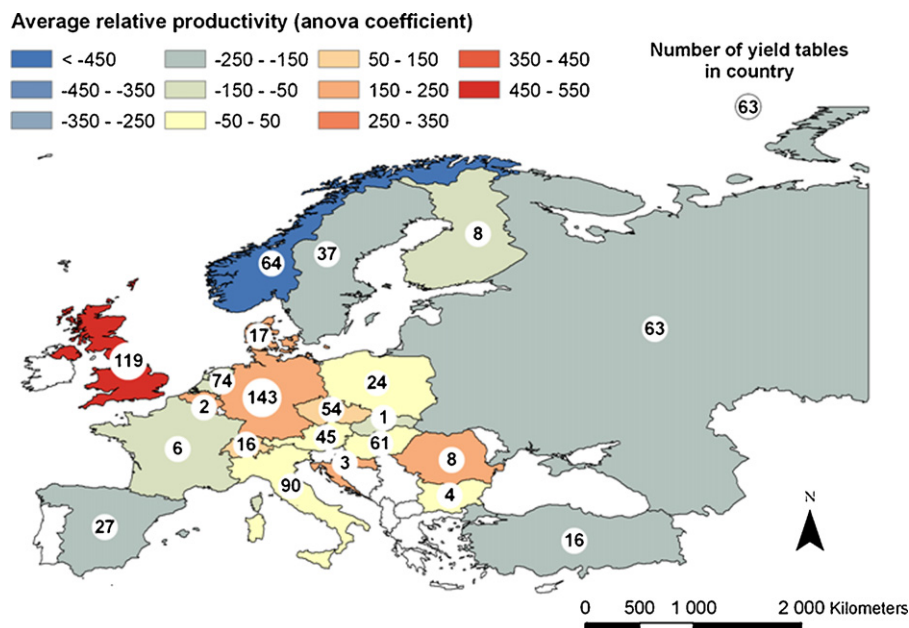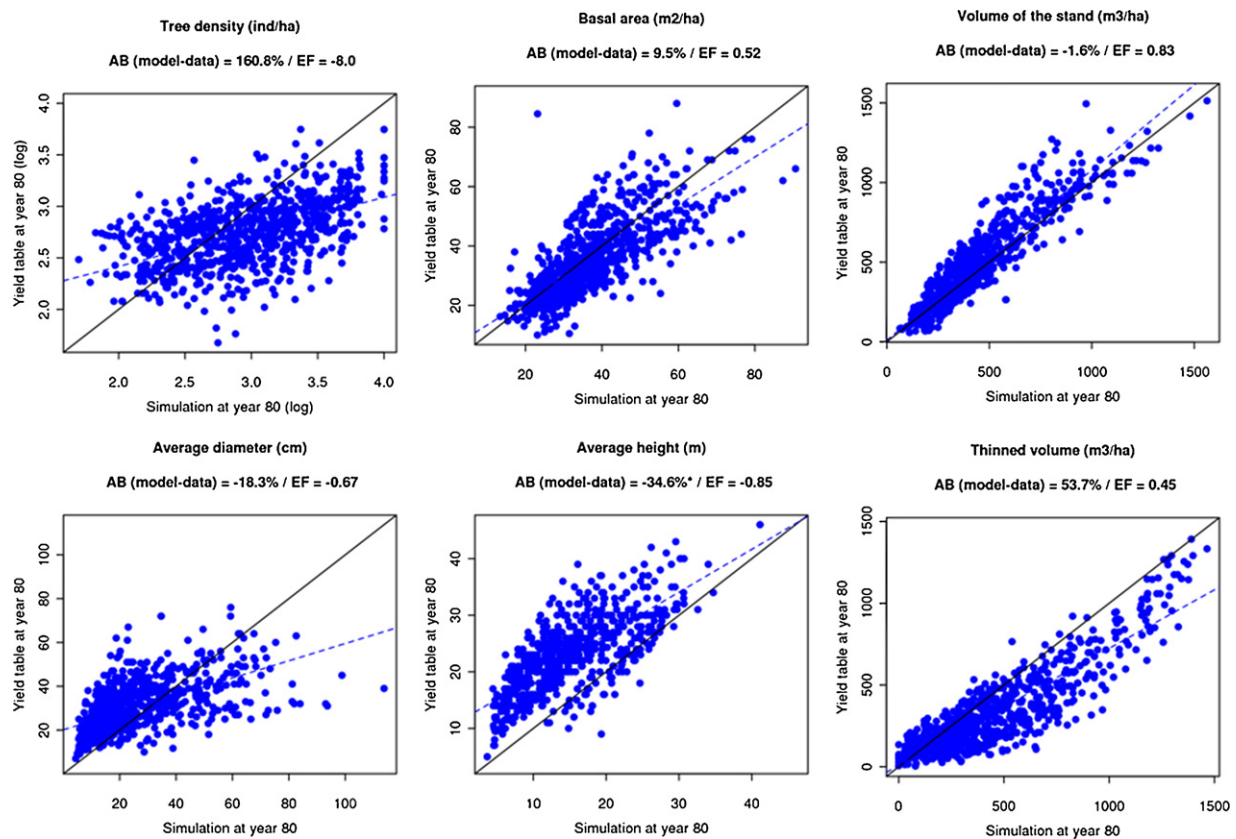

Fig. 5. Country productivity index based on the European yield table dataset. The "average relative productivity" index corresponds to the country-specific coefficient of the linear mixed model of Eq. (4). The studied variable is the volume increment at the age of 80, and the two explanatory variables are country and plant functional type.

Fig. 6. Validation of stand characteristics: YT_f simulation. Each blue dot corresponds the state of one permanent plot at its last measurement. The dotted blue line represents their linear regression. AB and EF are the average relative bias and model efficiency, respectively. An "*" indicates that the systematic error is higher than the unsystematic error ($RMSEs > RMSEu$). (For interpretation of the references to color in this figure legend, the reader is referred to the web version of the article.)

between PFTs and countries, this result points to a detectable effect of management style on tree density, although other explanations for the effect of PFT and country cannot be discarded (e.g., ecophysiological differences between PFTs and differences in methodology for establishing yield tables between countries). Similar results are obtained if density is replaced by basal area or standing volume in Eq. (5), showing that management styles also affect these two variables.

3.1.2.2. YT_f simulation: validation across a variety of management and climate conditions.
Except for tree density, average biases do not exceed 55% for the YT_f simulation, and most modelling efficiencies are higher than 0.3, with the exception of average height and average circumference (Figs. 6 and 7). The FMM performs particularly well for standing volume with an EF value of 0.83 and an average bias of only −2%. This value is slightly better than the "shadow model" (EF_{stat} = 0.82, AB_{stat} = 16%, see Table 2). Because standing volume varies little for a given level of total volume produced, the linear regression is indeed more sensitive to extreme values, which may differ between the calibration and test subsamples and produce a higher average bias in the shadow model.

For most variables, however, the performance of the FMM is lower for YT_f than under the highly controlled conditions of PP_f: efficiencies are lower and average biases are higher, as is the systematic to unsystematic error ratio; however, it remains below 1 for all variables except average height.

The FMM does not efficiently simulate tree density (EF = −8). In particular, it overestimates high densities. However, the average bias of +160% is not uniform: Fig. 6 shows that the fit is best for low densities (around 600 trees ha^{-1}), meaning that the average bias comes from the high number of data points from the high densi-

ties where the bias is particularly high, rather than a systematic bias spanning the entire density range. The average bias of +96% in the shadow model shows that reproducing the tree density trends from the yield tables is not easy to accomplish. This difficulty could originate from a specific treatment effect or measurement errors for the higher tree densities.

3.1.3. French national inventory
3.1.3.1. Interpolated NFI plots and NFI_{fmm} simulations: regional trends.
The interpolation technique unearths regional differences in volume increments (Fig. 8a and c), most of which are bolstered by a large number of plot measurements. For broadleaves, the range of the volume increment is from 2 to 18 m^3 ha^{-1} yr^{-1}, half that of the needleleaves, which can grow as fast as 30 m^3 ha^{-1} yr^{-1} in north-eastern France. In particular, regional lows of −48% and −59% in the Mediterranean region (2)[1] can be observed, extending somewhat inland toward south-central Toulouse to the west for broadleaves (3, −21%), and from the mid-Atlantic coast (7, −12% and −26%) to the Parisian basin for needleleaves (1, −10%). Robust regional highs occur in northeastern France (4, +36% for both) for both functional plant types, in Britanny (5, +5%) for needleleaves and at the southwestern tip (6, +15%) for broadleaves (Table 3).

The sign of these regional trends in volume increment is generally correctly simulated (see Table 4). However, the amplitude of these variations is often underestimated; in particular, the regional high in the north-eastern region (4) and the regional low for the

---

[1] To help readers unfamiliar with French geography, numbers between brackets refer to the regional markers of Fig. 8d. The exact boundaries of these "regions" are given in Figure S7 of Supplementary Materials.
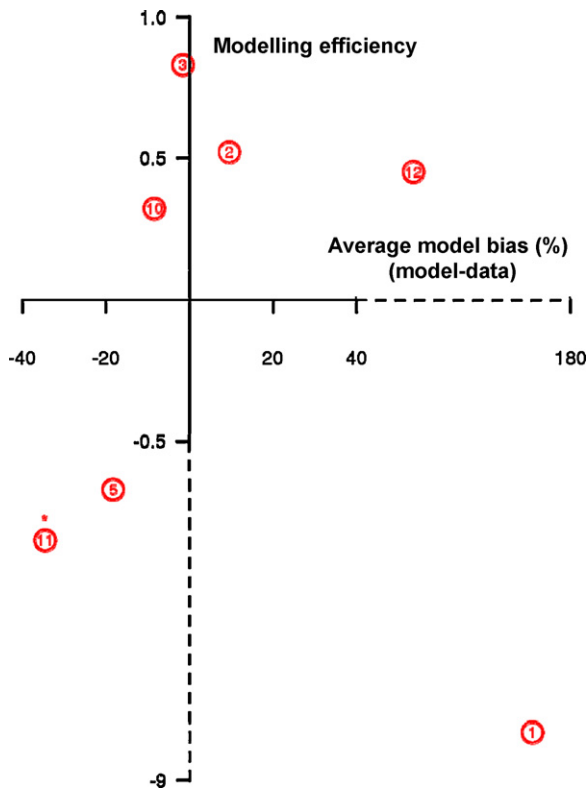
Fig. 7. Summary diagrams of model performance for the YT_f simulation. This diagram represents the model efficiency and average bias for a selected set of stand variables. An "*" indicates that the systematic error is higher than the unsystematic error ($RMSEs > RMSEu$). (1) Tree density, (2) basal area, (3) standing volume, (5) average circumference, (10) dominant height, (11) average height, (12) thinned volume.

Table 3

The FMM share of the total modelling error based on the permanent plots dataset (ES_{fmm}). For the definition of ES_{fmm}, see Eq. (11). Variable abbreviations: $dens$ (tree density), ba (basal area), vol_{main} (standing wood volume), av_{circ} (average circumference), $circ_{min}$ (minimum circumference), $circ_{max}$ (maximum circumference), σ (threshold circumference for basal area growth), γ (competition index).

Variable	ES_{fmm} (%)
$dens$	32%
ba	35%
vol_{main}	48%
av_{circ}	37%
$circ_{min}$	83%
$circ_{max}$	58%
σ	59%
γ	37%

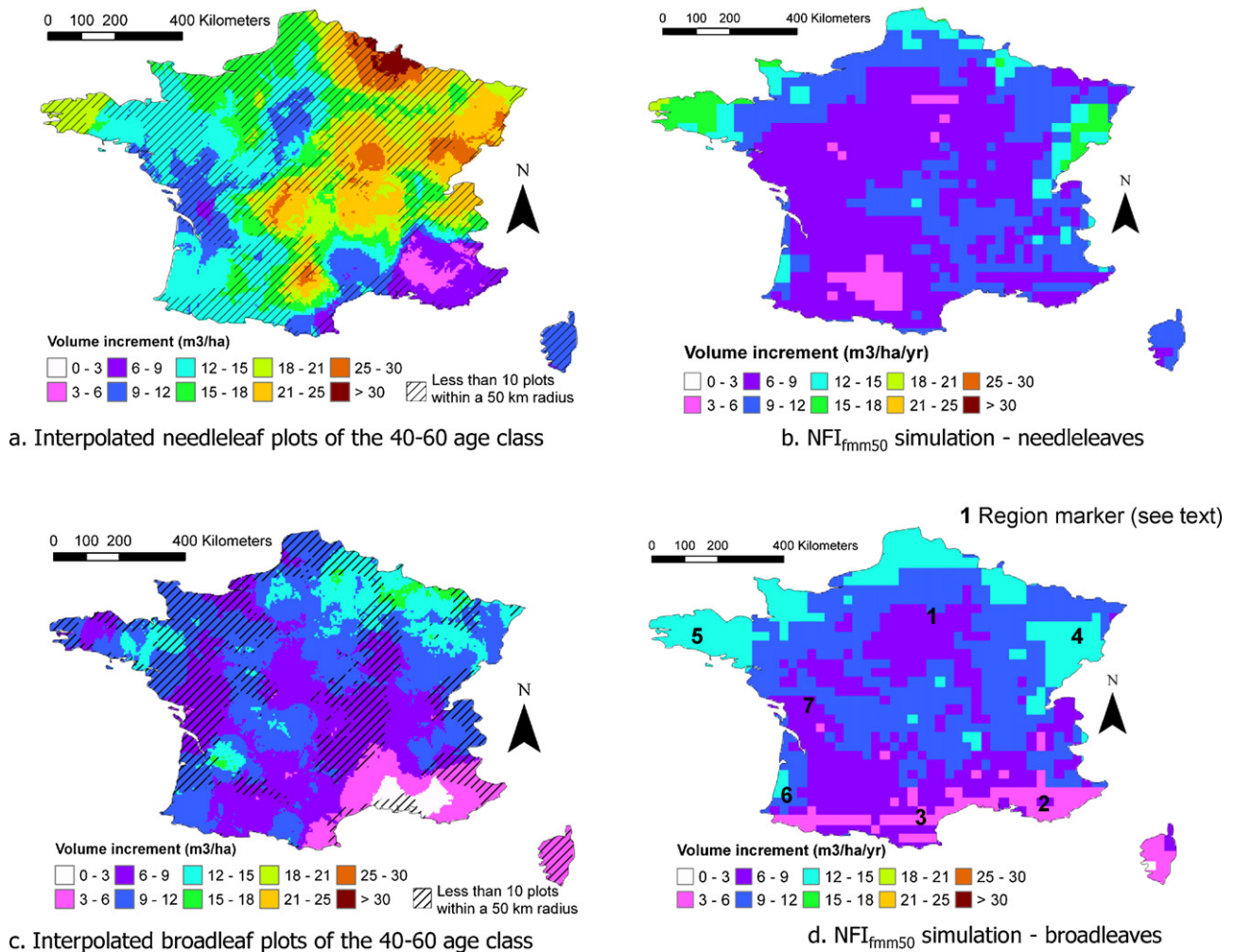Mediterranean (2) are both underestimated in the simulations (Fig. 8b and d).

3.1.3.2. Model fit for different age classes. Leaving the Mediterranean region aside, the simulated broadleaf increments are generally within the 20% uncertainty associated with the data-derived map (Fig. 9). The increment is, nevertheless, slightly underestimated around Paris and in the southwest, by 20% and 50%, respectively. On the contrary, needleleaf increments are systematically underestimated by at least 20% and often by more than 50% with the exception of the southwest (6). For both plant functional types, the volume increment is largely overestimated for the Mediterranean region.

3.1.3.3. Improvement in the simulation of biomass. For 50-year-old broadleaves, the standard version of ORCHIDEE (NFI_{std50}) overestimates standing volume, which is directly related to aboveground biomass stocks through wood density, by an average of 60% (Fig. 10a and c). ORCHIDEE-FM (NFI_{fmm50}) is much closer to the data (Fig. 10b), with an average underestimate of −16%. This pattern is also true for needleleaves at the southwestern tip of France (Fig. 11a). For the rest of the country except for the Mediterranean region, the standing volume is systematically underestimated. When productivity is optimised in NFI_{opt50}, model fit improves in some regions at the expense of others (Fig. 11b). The same happens when management is made more extensive with no artificial thinning (Fig. 11c). Only when productivity optimisation is combined with reduced management intensity in NFI_{opt_st50} can the high volumes measured in central and northeastern France be reproduced in the model (Fig. 11d). This result reflects the lesser intensiveness of management in these mountainous areas. A similar pattern in data-derived rdi confirms this interpretation (Figure S8).

3.2. Tree scale: individual tree growth and circumference distribution

3.2.1. Individual tree growth

The FMM model imperfectly reproduces individual tree growth variables as measured on the permanent plots (Fig. 12). Both σ and γ have low model efficiencies of 0.1 and −0.3, respectively, and γ is even significantly overestimated. However, both simulated variables vary within the correct range of values, and their average biases of around 15% are not alarmingly high given the low efficiencies. The relevant "shadow models" are also very inefficient, suggesting that the current input variables are not sufficient to correctly predict these variables. Thus, the simulation of σ and γ will be difficult to improve without a more detailed representation of inter-tree competition processes. This representation would require an additional level of complexity and site-specificity in

Table 4

Regional breakdown of the measured and simulated (IFN_{fmm50}) annual volume increment. The exact boundaries of these regions are given in Figure 6 of supplementary materials.

Region (label of Fig. 9d)	Broadleaves				Needleleaves			
	Volume increment (m³ ha⁻¹ yr⁻¹)		Relative difference to national average		Volume increment (m³ ha⁻¹ yr⁻¹)		Relative difference to national average	
	Measured	Simulated	Measured	Simulated	Measured	Simulated	Measured	Simulated
Parisian basin (1)	10.3	8.7	10%	−12%	15.2	6.8	−10%	−26%
Mediterranean (2)	3.8	6.2	−59%	−37%	8.8	9.0	−48%	−2%
Toulouse (3)	7.3	6.6	−21%	−34%	16.1	7.1	−5%	−23%
North-East (4)	12.7	12.0	36%	21%	23.0	11.3	36%	23%
Britanny (5)	9.2	14.2	−2%	44%	17.7	16.0	5%	74%
South-West (6)	10.8	9.0	15%	−9%	12.6	8.8	−26%	−4%
Mid-Atlantic (7)	8.3	8.6	−12%	−13%	12.3	7.3	−27%	−20%
France	9.4	9.9	0%	0%	16.9	9.2	0%	0%

Fig. 8. Validation of the volume increment at a regional scale. "Interpolated data" maps (a and c) are derived from National Forest Inventory plots, and "*NFI_{fmm50}* simulation" maps (b and d) represent the output of ORCHIDEE-FM simulations for 50-year-old stands.

the FMM, which is not compatible with the aimed generality of ORCHIDEE-FM.

3.2.2. Circumference distribution

When permanent plots are sorted by increasing the simulated proportion of trees in the greater than 1.4-m circumference category (Fig. 13), a similar trend toward larger circumference classes appears in the observed circumference distributions. This trend shows that the model can capture the inter-plot differences in circumference distribution. The trend in the data however, is blurred by several plots with a high proportion of narrower trees than simulated. Some of these are merely attenuated in the simulations (e.g., plots n°14-21-26), suggesting that circumference distribution is essentially driven by the volume increment, with the FMM slightly overestimating tree growth for lower values of the volume increment. In other cases, the high proportion of narrower trees is not simulated at all (e.g., plots N°6-46-47-55). In these cases, circumference distribution is probably driven by other factors that are not modelled in the FMM (e.g., a high level of competition for light due to local topography or a "from above" thinning strategy).

4. Discussion

4.1. Effect of climate and management on carbon stocks and fluxes

4.1.1. Regional assessment of carbon fluxes

The introduction of management and tree-level mortality into a GVM allows us to validate carbon stocks and stock changes on continuous maps derived from the spatially abundant inventory data. To our knowledge, this type of validation is a first for a GVM. It complements the validation of short-term CO_2 fluxes at flux towers. Although the inventory data only has a 5-year resolution in time, it uncovers regional variations in carbon fluxes that are very difficult to capture with flux towers. In particular, the low productivity of the Parisian basin and the high productivity of northeastern France that were detected in the data are correlated with pockets of low and high precipitation, respectively, in particular for the 5 years before 2006. The mixed performance of ORCHIDEE-FM in simulating these pockets is partly due to the mediocre accuracy of the climate forcing data: while the REMO reanalysis clearly shows a regional low in precipitation over the Parisian basin, it does not reproduce the pockets of higher precipitation in the northeast
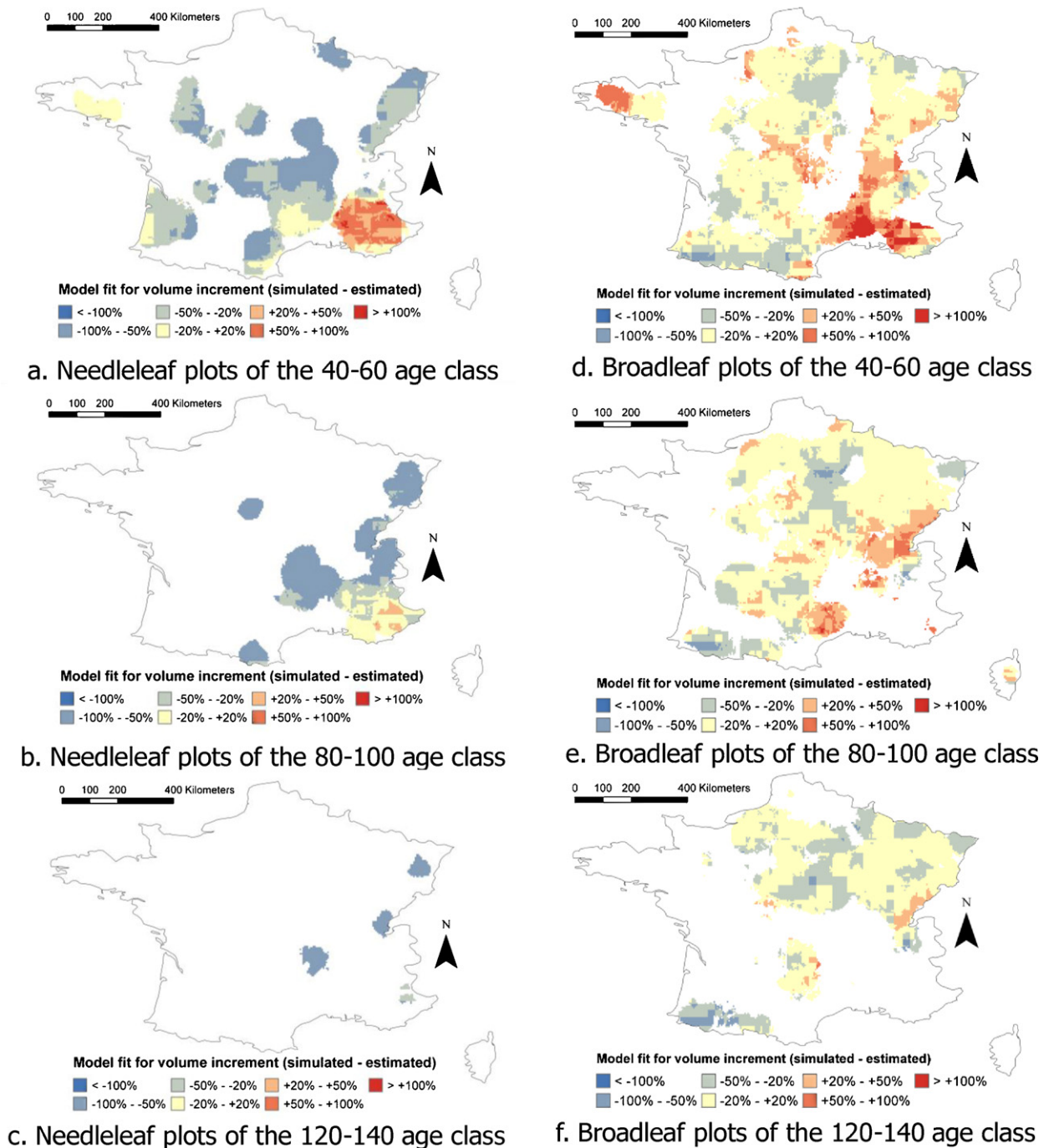
Fig. 9. Model fit for the volume increment: evolution with age. These 6 maps represent the model fit (($NFI_{fmm} - data$)/$data$) for the volume increment for three age classes of needleleaves (a, b, c) and broadleaves (d, e, f). White areas represent less than 10 data plots within a 55-km radius. Thus, the interpolation is considered too weak to assess model fit.

(Meteo-France, 2009). This shortcoming combined with a similar one in soil data (depth and texture) explains that simulations have a lower amplitude of spatial variation than averaged measurements. Another reason for this lower amplitude is the structure of the model itself. ORCHIDEE probably underestimates water stress in the Mediterranean context. In northeastern France, an area with high nitrogen deposition, the model's inability to simulate the high observed values in the volume increment partly comes from the absence of an explicit simulation of the nitrogen cycle.

Some larger-scale patterns, however, can be found in both the inventory and eddy-covariance data. Using eddy-covariance data, Luyssaert et al. (2007) found that precipitation drives NPP when average yearly temperature is higher than 10 °C. Because only a few mountainous grid cells (less than 10%) have an average temperature lower than 10 °C in France, this rule is consistent with our previous observation that precipitation drives most regional trends in the country, both in data-derived maps and simulations.

These comparisons between eddy-covariance-based and inventory-based validations must, nevertheless, be made cautiously. Flux towers measure whole-stand NEE (and GPP through flux-separation algorithms), while forest inventories estimate the share of NPP allocated to above-ground woody growth ($wood_{inc}$) over a time period of several years. Both variables are strongly correlated, but a model with a faulty allocation scheme could
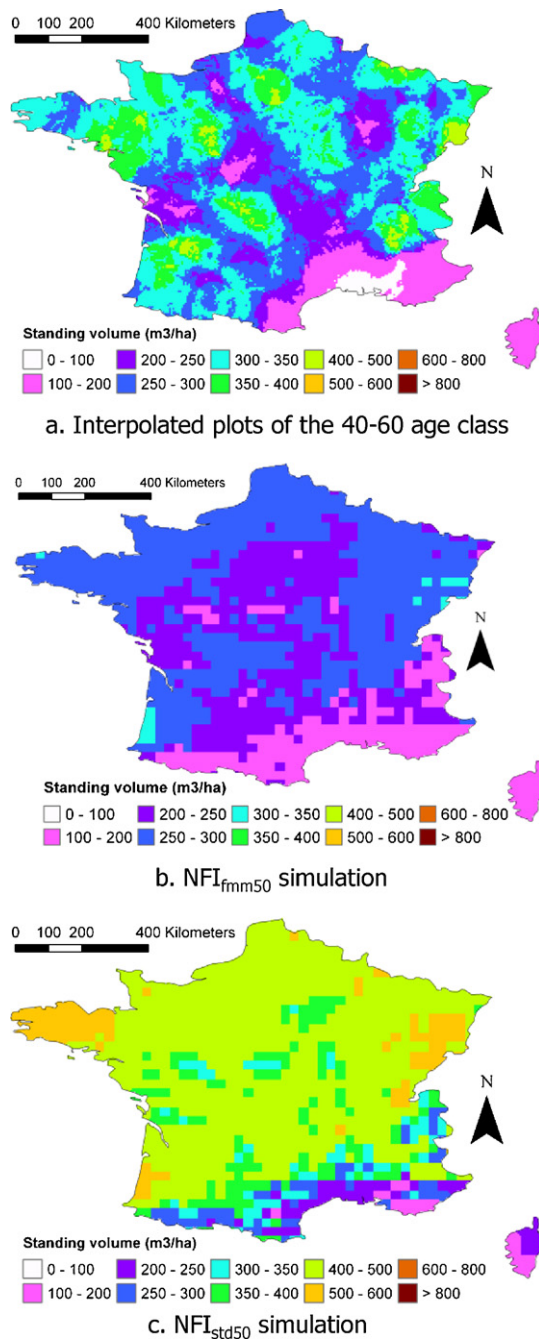
perform well for total GPP and badly for $wood_{inc}$. However, the joint use of both methods presents new opportunities for the separate validation of production and allocation processes.

4.1.2. Optimisation of biophysical parameters

Another key result from this spatially continuous validation is the rescaling from an optimisation of photosynthesis efficiency parameters for needleleaves. Using the optimised parameter values of Santaren (2006) improves model fit, but this does not prove sufficient for all regions: rescaling allocation, plant respiration or management intensity parameters also seem necessary. The model better reproduces the estimated standing volume in southwestern France, which is not surprising: the parameters of ORCHIDEE are based on published experimental studies, which are much more abundant for southwestern *Pinus pinaster* than for northeastern *Abies alba* and *Picea abies*. Our results question the generality of this parameterisation. Although this optimisation of maximum photosynthesis rates is very coarse, the results are qualitatively similar to the much finer GVM-oriented optimisation of vc_{max} using leaf nitrogen content that was carried out by Kattge et al. (2009). This optimisation was indeed an large upward correction from the original values of Beerling and Quick (1995) for temperate needleleaves (see Table 5).

4.1.3. Management intensity maps

Management variability has also been shown to be an important driver of stand characteristics and carbon stocks, both at regional (forest inventory) and continental (yield tables) scales. In particular, management intensity has been shown to play a comparable role to photosynthesis efficiency in explaining regional patterns of standing volume. This result suggests that the performance of GVMs could be significantly improved if management and photosynthesis efficiency were allowed to vary regionally instead of having unique PFT-specific parameterisation. Such a regional parameterisation would be feasible in Europe, where management intensity and species distribution can potentially be mapped (Nabuurs et al., 2008).

4.2. Simulating endogenous heterogeneity in a GVM

In the field of ecological modelling, a common distinction exists between exogenous heterogeneity, which arises from abiotic components such as climate or soil type, and endogenous heterogeneity, such as the heterogeneity in individual tree circumferences, which exists even in physically homogenous environments (Moorcroft et al., 2001). The validation of ORCHIDEE-FM highlight the use of simulating such fine-scale processes in large-scale GVMs. Although the endogenous heterogeneity now represented by the new model structure with extreme circumferences, competition indexes, and circumference distribution, is inefficiently simulated by ORHCIDEE-FM, the process-based model outperforms simple statistical models for stand-level variables such as basal area and standing volume. A similar pattern is found for the stand-level FORSKA model (Lindner et al., 1997). This similarity suggests that a correct average representation of endogenous heterogeneity is better than none at all, even if it poorly matches

Fig. 10. Standing volume of 50-year-old broadleaf stands. The "interpolated data" map (a) is derived from National Forest Inventory broadleaf plots of the 40–60-year age class and the "NFI_{fmm50} and NFI_{std50} simulation" maps (b and c) represent the output of ORCHIDEE-FM and ORCHIDEE simulations for 50-year-old broadleaf stands.

Table 5
Improved average vc_{max} values.

Plant functional type	Study	Improved vc_{max}	vc_{max} change from standard value
Temperate needleleaves	This study (ORCHIDEE model)	41.7	19%
	Kattge et al. (2009) (BETHY)	62.5	116%
Temperate broadleaves	This study (ORCHIDEE model)	55.0	0%
	Kattge et al. (2009) (BETHY)	57.7	65%
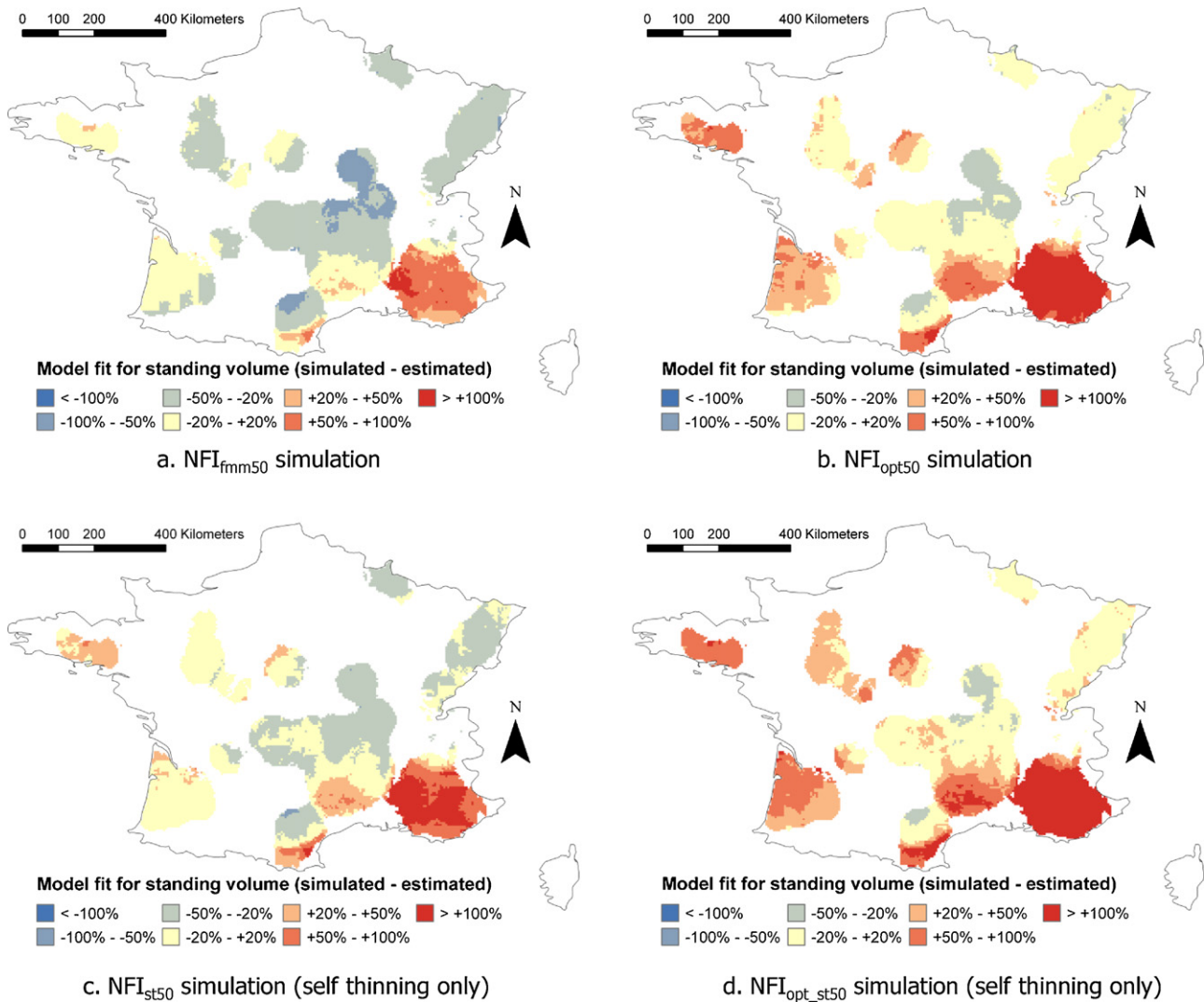
Fig. 11. Model fit for standing volume of 50-year-old needleleaf stands. These four maps represent the model fit (($NFI_{fmm} - data$)/$data$) for standing volume for four different simulation options: ORCHIDEE-FM (a), ORCHIDEE-FM with optimised photosynthesis efficiency (b), ORCHIDEE-FM without anthropogenic thinning (c) and ORCHIDEE-FM both with optimised photosynthesis efficiency and without anthropogenic thinning (d). White areas represent less than 10 data plots within a 55-km radius, and the interpolation is, therefore, considered too weak to assess model fit.

the data on a plot per plot basis. Moreover, the process-based simulation of endogenous heterogeneity presents the possibility to assess the impact of concrete management decisions, such as short rotations, high thinning intensity, and high thinning frequency, on carbon stocks and fluxes at large scales.

4.3. Model strengths and limitations

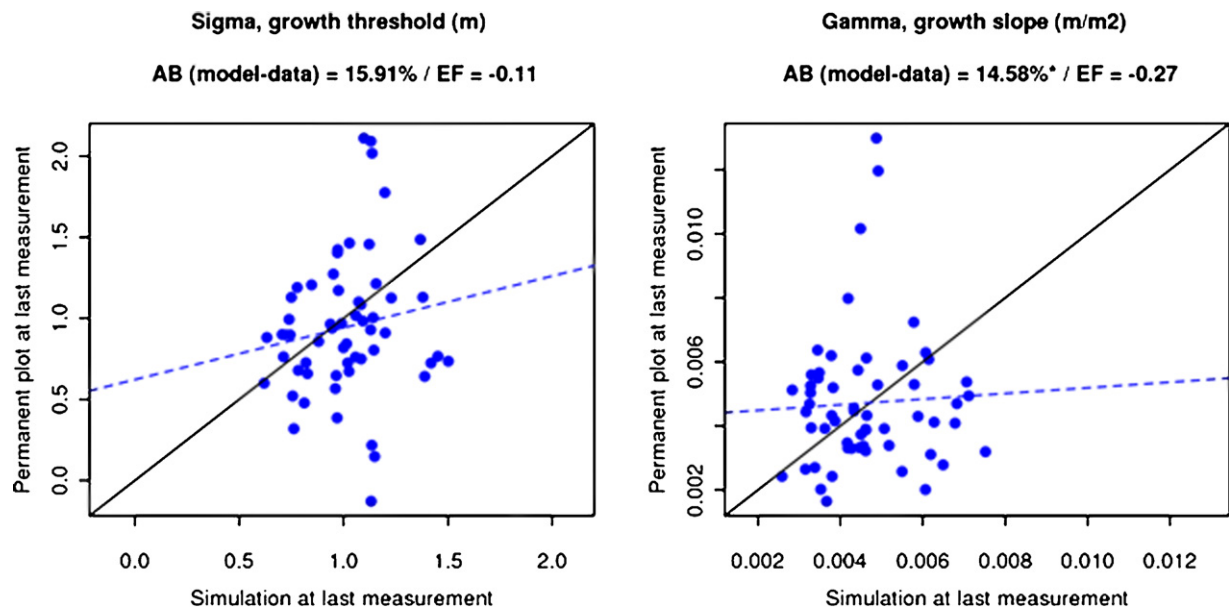#### 4.3.1. Model robustness for basal area and standing volume

The validation results for the yield tables show that despite a significant impact of management styles in the data, the simulations are quite efficient and not strongly biased, in particular, for standing volume and basal area. Similar conclusions can be drawn from the NFI_{fmm} simulations for broadleaf standing volume. The performance of ORCHIDEE-FM for basal area and standing volume probably has two explanations: first, the model is robust to changes in management parameters for these variables, as shown by the sensitivity analysis of Bellassen et al. (2010), and second, basal area and standing volume are less heavily influenced by local conditions than other variables such as average diameter or tree density and, therefore, respond more directly to the large-scale climatic variations driving GVMs like ORCHIDEE (Wang et al., 2006). Overall,

this robustness justifies the rationale for management simulation in GVMs, namely that simulating an "average" management is more realistic than not simulating management.

4.3.2. Tree density and self-thinning curves

The performance of ORCHIDEE-FM to simulate tree density and average diameter is much worse when the initial conditions and management style are unknown. The proportion of systematic error for these two variables is twice as high as for basal area or standing volume in the YT_f simulation, whereas they are comparable for all four variables in the PP_f simulation. There are two likely reasons for this systematic error:

- The self-thinning curves of ORCHIDEE-FM are not generic enough. Although Reineke (1933) originally thought that site or species productivity made no difference to his equations and would only accelerate the self-thinning process, this has recently been questioned (Yang and Titus, 2002; Vacchiano et al., 2008). Needle-leaves tolerate higher densities than broadleaves, thus suggesting an effect of at least plant functional type, if not species, on self-thinning curves (Fig. 14). For needleleaves, the default self-thinning curve of ORCHIDEE-FM seems to be generic enough

Sigma, growth threshold (m)

AB (model-data) = 15.91% / EF = −0.11

Gamma, growth slope (m/m2)

AB (model-data) = 14.58%* / EF = −0.27

Fig. 12. Validation of individual tree growth variables (σ and γ): PP_f simulation. Each blue dot corresponds to the state of one permanent plot at its last measurement. The dotted blue line represents their linear regression. *AB* and *EF* are average relative bias and model efficiency, respectively. An "*" indicates that the systematic error is higher than the unsystematic error (*RMSEs > RMSEu*). (For interpretation of the references to color in this figure legend, the reader is referred to the web version of the article.)

because it encompasses yield table data for the entire productivity range (total volume produced at year 80). However, this is not the case for broadleaves, for which many productive yield tables lie above the curve: some broadleaf species may, thus, be more tolerant to crowding than the oaks and beeches on which the self-thinning curve was established (Dhôte, 1999).

- The management style varies with density. Indeed, Fig. 14 suggests that management may be more intense when the stand is dense. For both plant functional types, the data-derived thinning curve cuts across the simulated values as the stand grows sparser.

Different management styles and intensities between European countries could explain the important variability of the data.

These results highlight the important contributions that empirical studies of self-thinning and thinning curves could make to the performance of ORCHIDEE-FM, which has already been shown to be very sensitive to these parameters (Bellassen et al., 2010). Another approach would be to construct a data assimilation framework for ORCHIDEE-FM to optimise the thinning and harvest parameters on existing wood production datasets.
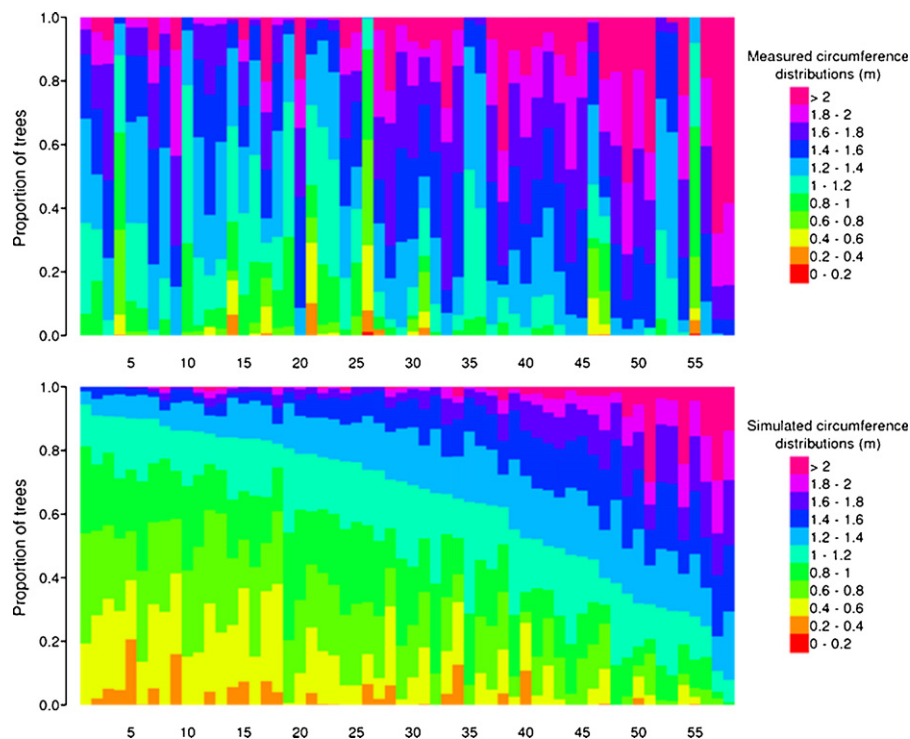
Fig. 13. Validation of circumference distribution: *PPf* simulation. The different hues indicate the repartition of trees between 11 circumference classes (ordinates) for the last measurement of each permanent plot (abscissa). Permanent plots were sorted by increasing the simulated proportion of trees in the greater than 1.4-m category.
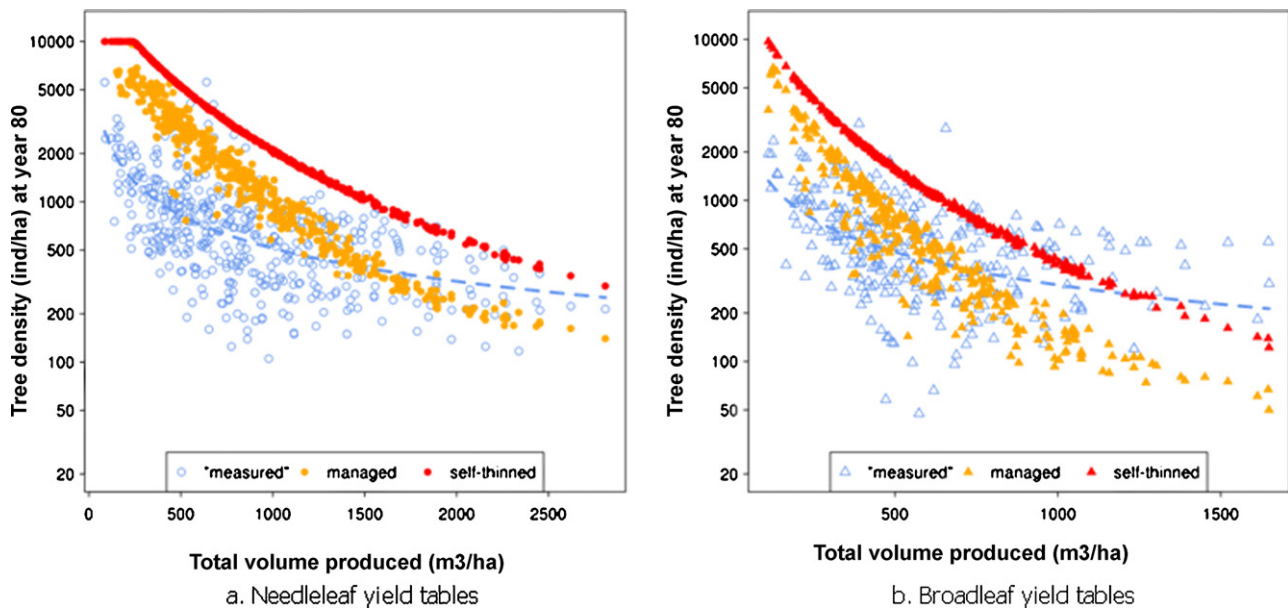
Fig. 14. Self-thinning curves based on yield tables. Full dots represent values of tree density against the total volume produced from the YT_f simulation (orange for a "managed" scenario and red for a "self-thinning only" scenario). Empty blue dots represent the corresponding data from yield tables, with a dashed line for the log-log linear regression. (For interpretation of the references to color in this figure legend, the reader is referred to the web version of the article.)

4.3.3. Bridging the gap with raw inventory data: basal area increment

One of the original ideas in ORCHIDEE-FM is its ability to put a process-based GVM on par with forest inventory data. In terms of proxy variables for productivity, ORCHIDEE-FM performs better for the volume increment than for the basal area increment. This is mainly due to the lack of performance of ORCHIDEE-FM at the tree scale: the basal area increment is very dependent on tree circumference distribution because many small trees will show a higher basal area increment than a few large trees for the same amount of volume increment. Therefore in this study, we used the estimated volume increment from the French inventory instead of the measured basal area increment. If the same validation exercise was undertaken at the European scale, then the basal area increment might be the only option because the methods for estimating volume vary strongly between countries, and a comparison based on the compilation of European forest inventories by Schelhaas et al. (2006) would be challenging without full documentation of each inventory's method. In this case, a possibility for improving the performance of ORCHIDEE-FM for the basal area increment would be to force the model for its initial conditions. If the model were fed with the measured tree circumference distribution before the productivity measurement by surface coring, ORCHIDEE-FM would be more reliable in its simulation of the basal area increment and would, therefore, provide a meaningful comparison with direct measurements.

5. Conclusion

The double aim of this study was to validate ORCHIDEE-FM at the various temporal and spatial scales necessary for a GVM and to separate the modelling error due to the simulation of management from that due to the simulation of productivity. We showed that ORCHIDEE-FM performs reasonably well over long time-scales for most stand-level variables (tree density, basal area, standing volume, average height, and average circumference) and at spatial scales varying from local to continental with several degrees of continuity between measurements. The performance of ORCHIDEE-FM is, however, less satisfying for fine-scale processes such as competition between trees. In terms of error separation, we showed that

when initial conditions and management style are controlled, the error from the FMM management component tends to be lower than that of the ORCHIDEE productivity component. However, the volume inventory data shows that both the management and the productivity components need to be calibrated if we want the model to finely reproduce the conditions of a specific region.

The validation of ORCHIDEE-FM also paves the way for its improvement. Specific attention should be paid to thinning parameters, either through more empirical studies or through an optimisation framework. The assimilation of initial conditions in the model could also present the possibility of a comparison with the raw measurements of forest inventories rather than the estimated volume and volume increment. Overall, ORCHIDEE-FM is deemed reliable enough to carry out prospective studies on the large-scale impact of management on climate and on the impact of climate change on business-as-usual management. In these applications, ORCHIDEE-FM will provide a useful complement to inventory-based studies because it allows the separation of the effects of CO_2, climate, and management on wood stocks and wood production.

Appendix A. List of abbreviations

AB	average bias
EF	modelling efficiency
FMM	forest management module

GPP   gross primary productivity
GVM   global vegetation model
HR   heterotrophic respiration
LAI   leaf area index
NEP   net ecosystem productivity
NFI   national forest inventory
NPP   net primary productivity
ORCHIDEE-FM name of the new version of the ORCHIDEE GVM,
         which includes a forest management module
PFT   plant functional type
PP   permanent plot
YT   yield table

Appendix C. Supplementary data

Supplementary data associated with this article can be found, in the online version, at doi:10.1016/j.ecolmodel.2010.08.038.

Appendix B. Summary of permanent plot characteristics.

ID	Department	Species	Age at last measurement year	First measurement year	Last measurement year	Post thinning relative density index	Size (ha)
1	Loir-et-Cher	oak	201	1927	2006	0.8	1
2	Allier	oak	153	1931	2003	0.5	1
3	Allier	oak	153	1931	2003	0.8	1
4	Meurthe-et-Moselle	mixed oak/beech	151	1904	2006	0.7	1
5	Meurthe-et-Moselle	oak	122	1959	2007	0.5	0.5
6	Meurthe-et-Moselle	oak	122	1959	2007	0.8	0.5
7	Seine-Maritime	beech	124	1931	2004	0.35	1
8	Seine-Maritime	beech	124	1931	2004	0.5	1
9	Seine-Maritime	beech	124	1931	2004	0.35	1
10	Seine-Maritime	beech	124	1931	2004	0.7	1
11	Orne	oak	165	1934	2005	0.8	1
12	Orne	oak	165	1934	2005	0.5	1
13	Meurthe-et-Moselle	beech	140	1904	1995	0.8	0.2
14	Meurthe-et-Moselle	beech	140	1904	1995	0.5	0.2
15	Meurthe-et-Moselle	beech	142	1904	1997	0.8	0.25
16	Meurthe-et-Moselle	beech	142	1904	1997	0.5	0.25
17	Meurthe-et-Moselle	beech	151	1904	2006	1	0.25
18	Aisne	beech	118	1922	1978	0.4	0.25
19	Aisne	beech	118	1922	1978	0.8	0.25
20	Aisne	beech	118	1922	1978	1	0.25
21	Aisne	beech	118	1922	1978	0.6	0.5
22	Allier	oak	183	1931	2003	0.7	1
23	Orne	oak	145	1933	2005	0.4	1
24	Meurthe-et-Moselle	beech	151	1904	2006	0.7	0.25
25	Meurthe-et-Moselle	mixed oak/beech	151	1904	2006	0.5	0.25
26	Meurthe-et-Moselle	beech	151	1904	2006	1	0.25
27	Aisne	beech	121	1922	2006	0.5	0.2
28	Aisne	beech	121	1922	2006	0.5	0.2
29	Aisne	beech	121	1922	2006	0.5	0.2
30	Aisne	beech	121	1922	2006	0.5	0.2
31	Vosges	beech	202	1923	1962	0.7	1
32	Meurthe-et-Moselle	oak	137	1928	2007	0.5	1
33	Meurthe-et-Moselle	oak	137	1928	2007	0.8	1
34	Meurthe-et-Moselle	beech	142	1904	1997	0.7	0.25
35	Orne	oak	113	1951	2005	0.8	1
36	Orne	oak	113	1951	2005	0.6	1
37	Orne	oak	113	1951	2005	0.4	1
38	Orne	oak	138	1934	2005	0.8	1
39	Orne	oak	138	1934	2005	0.5	1
40	Orne	oak	200	1934	1960	0.7	2
41	Loir-et-Cher	oak	181	1928	2006	0.8	1
42	Loir-et-Cher	oak	181	1928	2006	0.5	1
43	Loir-et-Cher	oak	146	1928	2006	0.8	1
44	Loir-et-Cher	oak	146	1928	2006	0.5	1
45	Allier	oak	98	1992	2003	0.8	0.5
46	Allier	oak	98	1992	2003	0.5	0.5
47	Aisne	beech	173	1922	1968	0.5	1
48	Aisne	beech	146	1922	2006	0.5	0.53
49	Allier	oak	203	1931	2003	0.7	2
50	Loir-et-Cher	oak	116	1966	2006	0.4	0.83
51	Loir-et-Cher	oak	116	1966	2006	0.4	0.47
52	Loir-et-Cher	oak	116	1966	2006	1	0.47
53	Loir-et-Cher	oak	116	1966	2006	0.8	1
54	Loir-et-Cher	oak	116	1966	2006	0.6	1
55	Orne	oak	188	1934	2005	0.9	1
56	Allier	oak	123	1959	2003	0.9	1
57	Allier	oak	123	1959	2003	0.7	1
58	Allier	oak	123	1959	2003	0.5	1

References

Abramowitz, G., Leuning, R., Clark, M., Pitman, A., 2008. Evaluating the performance of land surface models. Journal of Climate 21, 5468–5481.

Amiro, B.D., Orchansky, A.L., Barr, A.G., Black, T.A., Chambers, S.D., Chapin, F.S., Gouldenf, M.L., Litvakg, M., Liu, H.P., McCaughey, J.H., McMillan, A., Randerson, J.T., 2006. The effect of post-fire stand age on the boreal forest energy balance. Agricultural and Forest Meteorology 140, 41–50.

Baldocchi, D., Falge, E., Gu, L.H., Olson, R., Hollinger, D., Running, S., Anthoni, P., Bern-hofer, C., Davis, K., Evans, R., Fuentes, J., Goldstein, A., Katul, G., Law, B., Lee, X.H., Malhi, Y., Meyers, T., Munger, W., Oechel, W., Paw U, K.T., Pilegaard, K., Schmid, H.P., Valentini, R., Verma, S., Vesala, T., Wilson, K., Wofsy, S., 2001. FLUXNET: a new tool to study the temporal and spatial variability of ecosystem-scale carbon dioxide, water vapor, and energy flux densities. Bulletin of the American Meteorological Society 82, 2415–2434.

Beerling, D.J., Quick, W.P., 1995. A new technique for estimating rates of carboxy-lation and electron-transport in leaves of C-3 plants for use in dynamic global vegetation models. Global Change Biology 1, 289–294.

Bellassen, V., Le Maire, G., Dhote, J.F., Viovy, N., Ciais, P., 2010. Modeling forest man-agement within a global vegetation model—Part 1: Model structure and general behaviour. Ecological Modelling 221, 2458–2474.

Bottcher, H., Freibauer, A., Obersteiner, M., Schulze, E.D., 2008. Uncertainty analysis of climate change mitigation options in the forestry sector using a generic carbon budget model. Ecological Modelling 213, 45–62.

Carvalhais, N., Reichstein, M., Ciais, P., Collatz, G.J., Mahecha, M., Montagnani, L., Papale, D., Rambal, S., Seixas, J., 2010. Identification of vegetation and soil carbon pools out of equilibrium in a process model via eddy covariance and biometric constraints. Global Change Biology 16, 2813–2829.

Ciais, P., Schelhaas, M.J., Zaehle, S., Piao, S.L., Cescatti, A., Liski, J., Luyssaert, S., Le-Maire, G., Schulze, E.D., Bouriaud, O., Freibauer, A., Valentini, R., Nabuurs, G.J., 2008. Carbon accumulation in European forests. Nature Geoscience 1, 425–429.

Deleuze, C., Pain, O., Dhote, J.F., Herve, J.C., 2004. A flexible radial increment model for individual trees in pure even-aged stands. Annals of Forest Science 61, 327–335.

Demarty, J., Chevallier, F., Friend, A.D., Viovy, N., Piao, S., Ciais, P., 2007. Assimilation of global MODIS leaf area index retrievals within a terrestrial biosphere model. Geophysical Research Letters 34, 6.

Desai, A.R., Moorcroft, P.R., Bolstad, P.V., Davis, K.J., 2007. Regional carbon fluxes from an observationally constrained dynamic ecosystem model: impacts of distur-bance, CO$_2$ fertilization, and heterogeneous land cover. Journal of Geophysical Research-Biogeosciences, 112.

Dhôte, J.-F, Hervé, J.-C., 2000. Changements de productivité dans quatre forêts de chênes sessiles depuis 1930: une approche au niveau du peuplement. Annals of Forest Science 57, 651–680.

Dhôte, J.F., 1999. Compétition entre classes sociales chez le chêne sessile et le hêtre. Revue Forestière Française, 309–325.

Hurtt, G.C., Moorcroft, P.R., Pacala, S.W., Levin, S.A., 1998. Terrestrial models and global change: challenges for the future. Global Change Biology 4, 581–590.

IFN, 2006. Observer la forêt française: mission première de l'IFN. L'IF, p. 12.

IPCC, 2003. Good Practice Guidance for Land-Use, Land-Use Change and Forestry. Intergovernmental Panel on Climate Change, Kanagawa, Japan, p. 534.

IPCC, 2007. In: Team, C.W., Pachauri, R.K., Reisinger, A. (Eds.), Climate Change 2007: Synthesis Report. Contribution of Working Groups I, II and III to the Fourth Assessment Report of the Intergovernmental Panel on Climate Change, Inter-governmental Panel on Climate Change, Geneva, Switzerland, p. 104.

JRC, 2009. European Forest Yield Table's Database, http://afoludata.jrc.ec.europa.eu/DS_Free/abc_intro.cfm.

Jung, M., Le Maire, G., Zaehle, S., Luyssaert, S., Vetter, M., Churkina, G., Ciais, P., Viovy, N., Reichstein, M., 2007. Assessing the ability of three land ecosystem models to simulate gross carbon uptake of forests from boreal to Mediterranean climate in Europe. Biogeosciences 4, 647–656.

Kalnay, E., Kanamitsu, M., Kistler, R., Collins, W., Deaven, D., Gandin, L., Iredell, M., Saha, S., White, G., Woollen, J., Zhu, Y., Chelliah, M., Ebisuzaki, W., Higgins, W., Janowiak, J., Mo, K.C., Ropelewski, C., Wang, J., Leetmaa, A., Reynolds, R., Jenne, R., Joseph, D., 1996. The NCEP/NCAR 40-year reanalysis project. Bulletin of the American Meteorological Society 77, 437–471.

Kattge, J., Knorr, W., Raddatz, T., Wirth, C., 2009. Quantifying photosynthetic capacity and its relationship to leaf nitrogen content for global-scale terrestrial biosphere models. Global Change Biology 15, 976–991.

Krinner, G., Viovy, N., de Noblet-Ducoudre, N., Ogee, J., Polcher, J., Friedlingstein, P., Ciais, P., Sitch, S., Prentice, I.C., 2005. A dynamic global vegetation model for studies of the coupled atmosphere–biosphere system. Global Biogeochemical Cycles 19, 44.

Lanier, L., 1994. Précis de sylviculture. Ecole Nationale du Génie Rural, des Eaux et des Forêts (ENGREF), Nancy, p. 477.

Lindner, M., Lucht, W., Bouriaud, O., Green, T., Janssens, I., 2004. Specific Study on Forest Greenhouse Gas Budget. CarboEurope-GHG, Jena, p. 62.

Lindner, M., Sievanen, R., Pretzsch, H., 1997. Improving the simulation of stand structure in a forest gap model. Forest Ecology and Management 95, 183–195.

Loustau, D., 2004. Rapport final du projet CARBOFOR. INRA, Bordeaux, p. 138.

Luyssaert, S., Inglima, I., Jung, M., Richardson, A.D., Reichsteins, M., Papale, D., Piao, S.L., Schulzes, E.D., Wingate, L., Matteucci, G., Aragao, L., Aubinet, M., Beers, C., Bernhoffer, C., Black, K.G., Bonal, D., Bonnefond, J.M., Chambers, J., Ciais, P., Cook, B., Davis, K.J., Dolman, A.J., Gielen, B., Goulden, M., Grace, J., Granier, A., Grelle, A., Griffis, T., Grunwald, T., Guidolotti, G., Hanson, P.J., Harding, R., Hollinger, D.Y., Hutyra, L.R., Kolar, P., Kruijt, B., Kutsch, W., Lagergren, F., Laurila, T., Law, B.E., Le Maire, G., Lindroth, A., Loustau, D., Malhi, Y., Mateus, J., Migliavacca, M., Misson, L., Montagnani, L., Moncrieff, J., Moors, E., Munger, J.W., Nikinmaa, E., Ollinger, S.V., Pita, G., Rebmann, C., Roupsard, O., Saigusa, N., Sanz, M.J., Seufert, G., Sierra, C., Smith, M.L., Tang, J., Valentini, R., Vesala, T., Janssens, I.A., 2007. CO$_2$ balance of boreal, temperate, and tropical forests derived from a global database. Global Change Biology 13, 2509–2537.

Masek, J.G., Collatz, G.J., 2006. Estimating forest carbon fluxes in a disturbed southeastern landscape: integration of remote sensing, forest inventory, and biogeochemical modeling. Journal of Geophysical Research 111, G01006.

Meteo-France, 2009. Précipitations annuelles (en mm), période 1961–1990, http://www.languedoc-roussillon.ecologie.gouv.fr/.

Moorcroft, P.R, Hurtt, G.C., Pacala, S.W., 2001. A method for scaling vegetation dynamics: the Ecosystem Demography model (ED). Ecological Monographs 71, 557–585.

Nabuurs, G.J., Hengeveld, G., Heidema, N., Brus, D., Goedhart, P., Walvoort, D., van den Wyngaert, I., van der Werf, B., Tröltzsch, K., Lindner, M., Zanchi, G., Gal-laun, H., Schwaiger, H., Teobaldelli, M., Seufert, G., Kenter, B., 2008. Mapping the Continent: High Resolution Forest Resource Analyses of European Forests. CarboEurope-IP, p. 4.

Nagy, M.T., Janssens, I.A., Yuste, J.C., Carrara, A., Ceulemans, R., 2006. Footprint adjusted net ecosystem CO$_2$ exchange and carbon balance components of a temperate forest. Agricultural and Forest Meteorology 139, 344–360.

Oreskes, N., Shraderfrechette, K., Belitz, K., 1994. Verification, validation, and con-firmation of numerical-models in the earth-sciences. Science 263, 641–646.

Reichstein, M., Ciais, P., Papale, D., Valentini, R., Running, S., Viovy, N., Cramer, W., Granier, A., Ogee, J., Allard, V., Aubinet, M., Bernhofer, C., Buchmann, N., Carrara, A., Grunwald, T., Heimann, M., Heinesch, B., Knohl, A., Kutsch, W., Loustau, D., Manca, G., Matteucci, G., Miglietta, F., Ourcival, J.M., Pilegaard, K., Pumpanen, J., Rambal, S., Schaphoff, S., Seufert, G., Soussana, J.F., Sanz, M.J., Vesala, T., Zhao, M., 2007. Reduction of ecosystem productivity and respiration during the European summer 2003 climate anomaly: a joint flux tower, remote sensing and modelling analysis. Global Change Biology 13, 634–651.

Reineke, L.H., 1933. Perfecting a stand-density index for even-aged forests. Journal of Agricultural Research 46, 627–638.

Rykiel, E.J., 1996. Testing ecological models: the meaning of validation. Ecological Modelling 90, 229–244.

Santaren, D., 2006. Optimisation des paramètres du modèle de biosphère ORCHIDEE à partir de mesures sur site des flux de carbone, d'eau et d'énergie. Université Versailles Saint-Quentin, Versailles, p. 190.

Sato, H., Itoh, A., Kohyama, T., 2007. SEIB-DGVM: a new dynamic global vegetation model using a spatially explicit individual-based approach. Ecological Modelling 200, 279–307.

Schaefer, K., Collatz, G.J., Tans, P., Denning, A.S., Baker, I., Berry, J., Prihodko, L., Suits, N., Philpott, A., 2008. Combined Simple Biosphere/Carnegie-Ames-Stanford Approach terrestrial carbon cycle model. Journal of Geophysical Research-Biogeosciences 113, 13.

Schelhaas, M.J., Varis, S., Schuck, A., Nabuurs, G.J., 2006. EFISCEN Inventory Database, http://www.efi.int/portal/virtual_library/databases/efiscen/.

Smith, P., Powlson, D.S., Smith, J.U., Elliott, E.T., 1997. Special issue – evaluation and comparison of soil organic matter models using datasets from seven long-term experiments – preface. Geoderma 81, 1–3.

Soares, P., Tome, M., Skovsgaard, J.P., Vanclay, J.K., 1995. Evaluating a growth model for forest management using continuous forest inventory data. Forest Ecology and Management 71, 251–265.

Thornton, P.E., Law, B.E., Gholz, H.L., Clark, K.L., Falge, E., Ellsworth, D.S., Golstein, A.H., Monson, R.K., Hollinger, D., Falk, M., Chen, J., Sparks, J.P., 2002. Modeling and measuring the effects of disturbance history and climate on carbon and water budgets in evergreen needleleaf forests. Agricultural and Forest Meteorology 113, 185–222.

Turner, D.P., Ritts, W.D., Cohen, W.B., Maeirsperger, T.K., Gower, S.T., Kirschbaum, A.A., Running, S.W., Zhao, M.S., Wofsy, S.C., Dunn, A.L., Law, B.E., Campbell, J.L., Oechel, W.C., Kwon, H.J., Meyers, T.P., Small, E.E., Kurc, S.A., Gamon, J.A., 2005. Site-level evaluation of satellite-based global terrestrial gross primary production and net primary production monitoring. Global Change Biology 11, 666–684.

Urbanski, S., Barford, C., Wofsy, S., Kucharik, C., Pyle, E., Budney, J., McKain, K., Fitz-jarrald, D., Czikowsky, M., Munger, J.W., 2007. Factors controlling CO$_2$ exchange on timescales from hourly to decadal at Harvard Forest. Journal of Geophysical Research-Biogeosciences, 112.

Vacchiano, G., Motta, R., Long, J.N., Shaw, J.D., 2008. A density management diagram for Scots pine (Pinus sylvestris L.): a tool for assessing the forest's protective effect. Forest Ecology and Management 255, 2542–2554.

Vetter, M., Churkina, G., Jung, M., Reichstein, M., Zaehle, S., Bondeau, A., Chen, Y., Ciais, P., Feser, F., Freibauer, A., Geyer, R., Jones, C., Papale, D., Tenhunen, J., Tomel-leri, E., Trusilova, K., Viovy, N., Heimann, M., 2008. Analyzing the causes and spatial pattern of the European 2003 carbon flux anomaly using seven models. Biogeosciences 5, 561–583.

Viovy, N., Calvet, J.C., Ciais, P., Dolman, A.J., Gusev, Y., El Mayaar, M., Moors, E., Nasanova, O., Pitman, A., Polcher, J., Rivalland, V., Shmakin, A., Verseghy, D., 2010. The PILPS-CARBON model evaluation experiment: a test bed for simu-lating water, energy and carbon exchange over a forest canopy. Manuscript in preparation.

Wang, X., Fang, J., Tang, Z., Zhu, B., 2006. Climatic control of primary forest structure and DBH-height allometry in Northeast China. Forest Ecology and Management 234, 264.

Willmott, C.J., 1982. Some comments on the evaluation of model performance. Bulletin of the American Meteorological Society 63, 1309–1313.

Yang, Y., Titus, S.J., 2002. Maximum size-density relationship for constraining individual tree mortality functions. Forest Ecology and Management 168, 259–273.

Zaehle, S., Sitch, S., Prentice, I.C., Liski, J., Cramer, W., Erhard, M., Hickler, T., Smith, B., 2006. The importance of age-related decline in forest NPP for modeling regional carbon balances. Ecological Applications 16, 1555–1574.